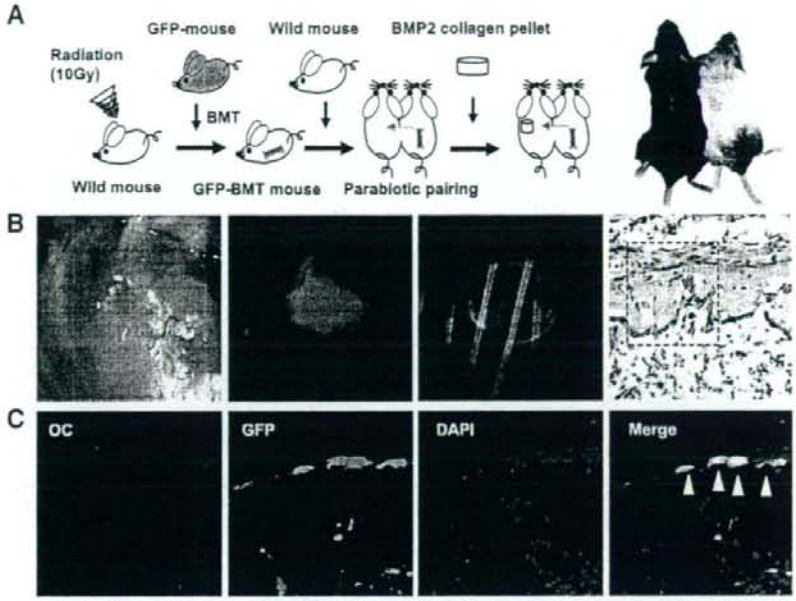

Figure 1. Bone marrow-derived osteoblast progenitor cells contribute to BMP-2-induced ectopic bone formation via circulation in a parabiotic mouse. **(A):** Parabiotic pairing between a GFP-BMT mouse and a wild-type mouse. A BMP-2 pellet was implanted into the wild-type mouse that could receive GFP-positive bone marrow cells from the GFP-BMT mouse through the circulation. **(B):** A BMP-2 pellet showed accumulation of GFP fluorescence 3 weeks after implantation under the muscular fascia of a wild-type parabiotic mouse. A soft x-ray photo of the BMP-2 pellet 3 weeks after the implantation demonstrated that ectopic bone formed in the BMP-2 pellet. Histologic section stained with H&E of the BMP-2 pellet 3 weeks after implantation also revealed bone formation in the BMP-2 pellet. Magnification, ×200. **(C):** Immunofluorescence staining of the boxed region in the H&E section showed that the cells lining the newly generated bone were osteoblasts expressing OC. Some of those osteoblasts expressing osteocalcin also exhibited GFP fluorescence (arrowheads). Magnification, ×600. Abbreviations: BMP, bone morphogenetic protein; BMT, bone marrow transplantation; DAPI, 4′,6-diamidino-2-phenylindole; GFP, green fluorescent protein; OC, osteocalcin.

If both mice provide the bone marrow cells equally, these data suggest that approximately 50% of the regenerating osteoblasts may be derived from endogenous circulating MOPCs in parabiotic mice.

CD45-Negative Fraction in Bone Marrow Is a Major Source of Circulating MOPCs

We next examined a particular population in bone marrow to determine the major source of the circulating MOPCs. To determine whether the major source of MOPCs in bone marrow is CD45-positive or CD45-negative, we transplanted two types of bone marrow cells in combination to a lethally irradiated mouse before BMP-2-pellet implantation: a combination of CD45-negative/GFP-negative bone marrow cells and CD45-positive/GFP-positive bone marrow cells to generate CD45/GFP-BMT (Fig. 2A). The ectopic bone formed in the CD45/GFP-BMT mouse showed less accumulation of GFP fluorescence than that in the GFP-BMT mouse (Fig. 2B, 2C). Histologic examination revealed that the transplanted cells with a reduced CD45-negative/GFP-positive fraction formed ectopic bone with significantly fewer GFP-positive osteoblasts (11.0% ± 3.4%) than the controls (43.4% ± 10.6%, $p = .00127$; Fig. 2D). These data suggested that CD45-negative cells in bone marrow might be the major source of circulating MOPCs in BMP-2-implanted mice, although the contribution of CD45-positive cells to ectopic bone formation can not be completely excluded.

Kinetic Analysis of Circulating MOPCs

The data obtained led us to further characterize the kinetics of CD45-negative cell migration from bone marrow to circulating blood. To view CD45-negative cells in the circulation, five sets of the experiment were performed independently. In each experiment, seven mice were serially implanted (i.e., one mouse per day) with a BMP-2 pellet, and at day 7, they were all at once subjected to flow cytometry analysis to evaluate the CD45-negative cell populations in the PBMNCs. Before the implantation, the basal population of the CD45-negative cells in PBMNCs was less than 20%, possibly containing a remnant fraction of red blood cells even after the conventional PBMNC isolation procedure. Surprisingly, large increases of the CD45-negative population in PBMNCs, up to 83% frequency, were observed within 7 days after BMP-2-pellet implantation, coinciding with a significant reduction in the CD45-negative population in bone marrow cells within 7 days after BMP-2 implantation (Fig. 3A). A similar increase in the CD45-negative population in PBMNCs was observed at least once within 7 days after BMP-2-implantation in the other four sets of experiments. The induction of CD45-negative population in PBMNCs at the peak in each set of experiments was significantly higher in the BMP-2-implanted mice than in the control mice ($p = .0000142$; Fig. 3B). Implantation of empty collagen pellets also showed a relatively smaller but significant induction of the CD45-negative population in PBMNCs at the peak ($p = .0198$; Fig. 3B).

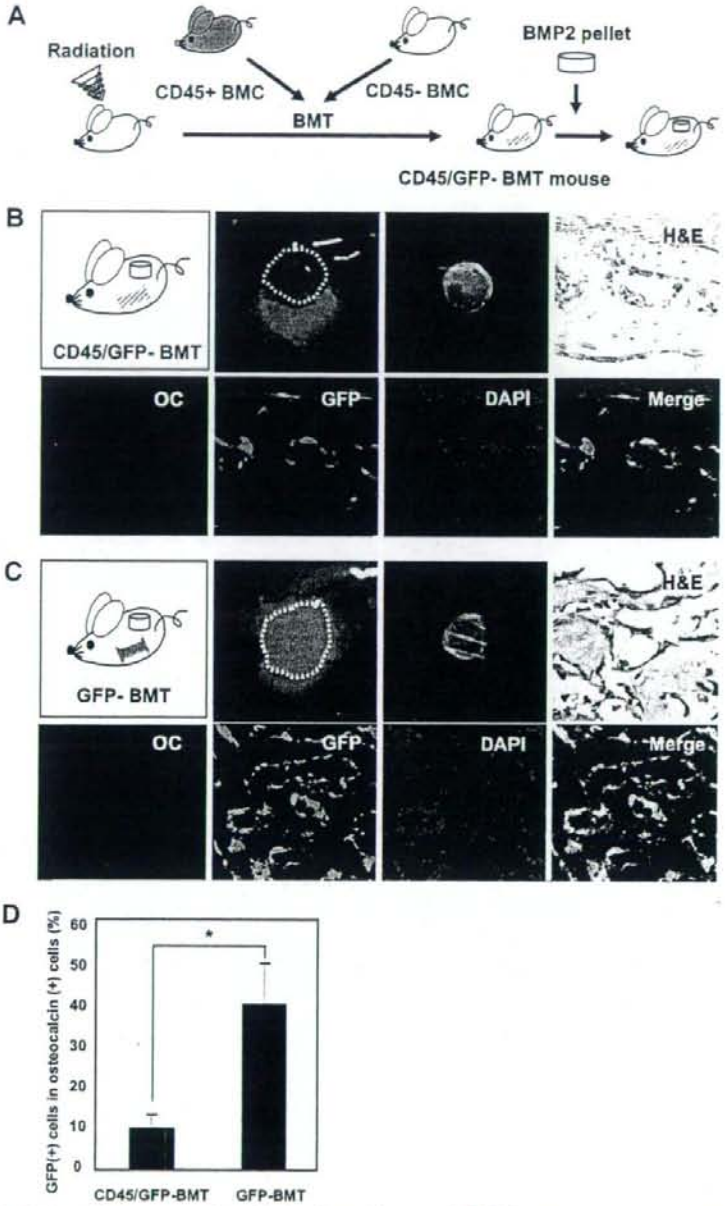

Figure 2. CD45-negative fraction of bone marrow cells predominantly participated in the BMP-2-induced ectopic bone formation. **(A):** CD45-negative bone marrow cells from wild-type mice and CD45-positive bone marrow cells from GFP-transgenic mice were transplanted into a lethal-dose-irradiated wild-type mouse (CD45/GFP-BMT) before the BMP-2-pellet implantation. **(B):** The ectopic bone (circled with a dotted line) in the CD45/GFP-BMT mouse showed weak GFP fluorescence. A soft x-ray photo and H&E-stained histologic section showed successful ectopic bone formation in the CD45/GFP-BMT mice. Immunofluorescence staining revealed fewer GFP-positive cells in the ectopic bone of the CD45/GFP-BMT mice than in the ectopic bone of the GFP-BMT mice. Magnification, ×400. **(C):** Total bone marrow cells from GFP transgenic mice were transplanted to lethally irradiated wild-type mice (GFP-BMT mouse). A BMP-2 pellet in the GFP-BMT mouse showed stronger GFP fluorescence (circled with a dotted line). A soft x-ray photo and histologic H&E-stained section showed bone formation in the BMP-2 pellet in the GFP-BMT mice as well. Immunofluorescence staining revealed that more GFP-positive cells expressed OC in the newly formed bone. Magnification, ×200. **(D):** Quantitative analysis showed that the percentage of GFP-positive/osteocalcin-positive osteoblasts in the osteocalcin-positive osteoblasts lining the trabecular bone significantly decreased in the CD45/GFP-BMT mice compared with the GFP-BMT mice. *, $p = .00127$. Abbreviations: BMC, bone marrow cell; BMP, bone morphogenetic protein; BMT, bone marrow transplantation; DAPI, 4',6-diamidino-2-phenylindole; GFP, green fluorescent protein; OC, osteocalcin.

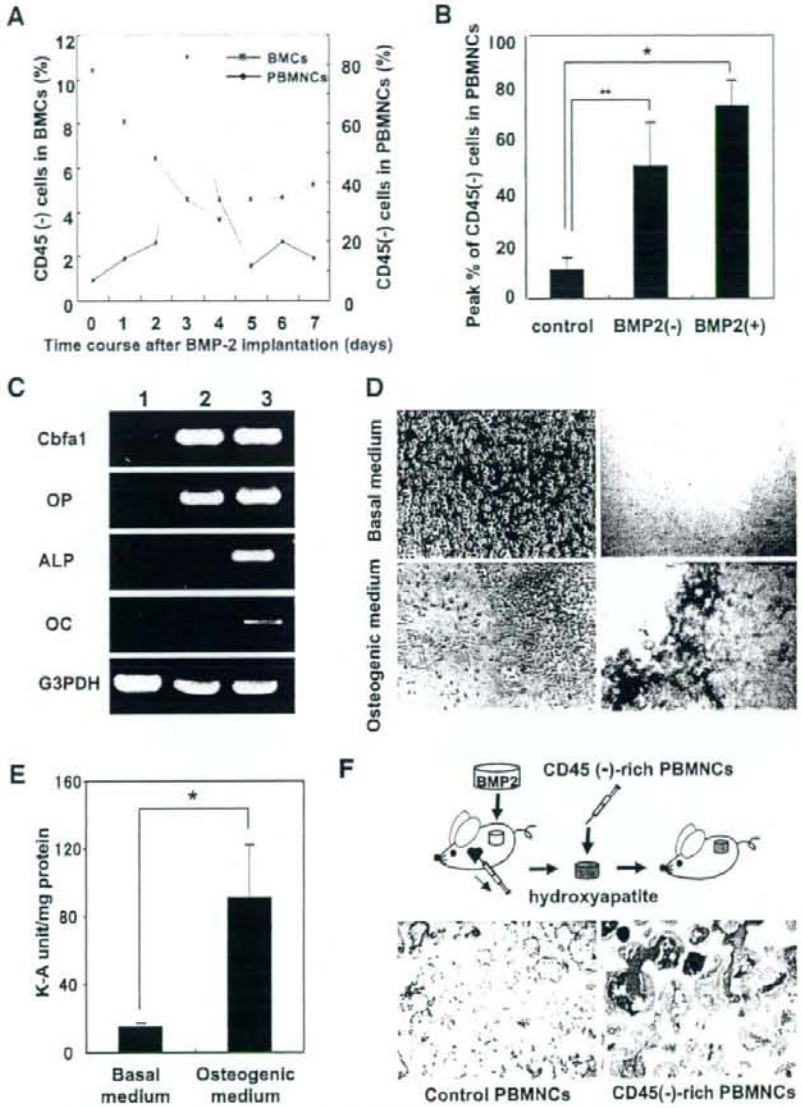

Figure 3. MOPCs were detected in PBMNCs from BMP-2 pellet-implanted mice. **(A):** Representative results of time-course analysis of five different sets of experiments. The CD45-negative cell population (%) in PBMNCs and BMCs of the BMP-2-implanted mice was analyzed with flow cytometry for 7 days after BMP-2 implantation. Robust but transient appearance of a CD45-negative population in PBMNCs according to the significant reduction of the CD45-negative population in BMCs within 7 days after BMP-2-implantation was observed in five different sets of experiments compared with nontreated wild-type mice (day 0). **(B):** Analysis of average percentage of CD45-negative population in PBMNCs at peak time within 7 days after BMP-2 implantation in five different sets of experiments showed that the CD45-negative population in PBMNCs was significantly induced by BMP-2-pellet implantation. *, $p = .0000142$. **(C):** Reverse transcription-polymerase chain reaction analysis of the magnetic cell sorting-sorted CD45-negative PBMNCs showed that these cells exhibited Cbfa1 expression before culture (lane 1), additional OP expression in culture without BMP-2 stimulation (lane 2), and ALP and OC expression in culture with BMP-2 stimulation for 3 weeks (300 ng/ml; lane 3). **(D):** The sorted CD45-negative cells cultured in basal medium and in osteogenic medium for 4 weeks showed morphogenic changes to osteoblastic features. Magnification, ×40. Alizarin red staining (right panels) showed that calcium deposition was observed only in cells cultured in osteogenic medium. Magnification, ×40. **(E):** ALP assay showed that ALP activity was increased when the CD45-negative cells in PBMNCs were cultured in osteogenic medium. **(F):** Histologic H&E-stained sections of the hydroxyapatite transplanted in vivo with (right) or without (left) the CD45-negative cells in PBMNCs revealed that those cells could form bone in hydroxyapatite. Magnification, ×100. Abbreviations: ALP, alkaline phosphatase; BMC, bone marrow cell; BMP, bone morphogenetic protein; G3PDH, glyceraldehyde-3-phosphate dehydrogenase; K-A, King-Armstrong; OC, osteocalcin; OP, osteopontin; PBMNC, peripheral blood mononuclear cell.

To determine whether the mobilized CD45-negative cells in the circulation contained MOPCs, we enriched the CD45-negative fraction of the PBMNCs with MACS. The CD45-negative sorted cells already expressed Cbfa1 (Fig. 3C). We cultured the sorted cells in basal medium and examined the expression of osteoblast-specific mRNA in these cells with or without BMP-2 stimulation for 3 weeks. Osteopontin (OP), an early marker of mesenchymal differentiation, started to be expressed in cultures without BMP-2 (Fig. 3C). As expected, the addition of BMP-2 to the culture (300 ng/ml) efficiently induced the expression of osteoblast-specific marker genes such as ALP and OC (Fig. 3C). These results coincided with the data at the protein level that we reported previously [11]. We also observed morphological and functional changes of the CD45-negative sorted cells cultured in the osteogenic medium for 4 weeks. Those cells showed morphologic changes with osteoblastic features, and calcium deposition was clearly observed by alizarin red staining (Fig. 3D). A significant increase in ALP activity was also demonstrated (Fig. 3E). To obtain further evidence of the osteogenic potential of the circulating CD45-negative cells in vivo, we transplanted the fully open interconnected porous calcium hydroxyapatite with or without the cultured circulating CD45-negative cells from GFP-transgenic mice under the muscular fascia in the backs of nude mice (Fig. 3F). Eight weeks later, the hydroxyapatite was harvested and histologically analyzed. Newly formed bone was clearly seen only in the hydroxyapatite with the inoculated CD45-negative cells (Fig. 3F). Immunofluorescence staining showed that the cells in the newly formed bone were GFP-positive, suggesting that not the cells from recipient nude mouse but the transplanted cells with the hydroxyapatite had formed the bone (supplemental online Fig. 2). These data indicate that CD45-negative cells mobilized from bone marrow to the circulating blood contain a major, if not exclusive, population of MOPCs that are derived from bone marrow and provide mature osteoblasts to peripheral tissues.

Characterization of Circulating MOPCs

We further analyzed cell surface markers of the circulating MOPCs in PBMNCs by flow cytometry analysis (Fig. 4). Significant expression of CD44, which is expressed in mesenchymal cells as a receptor of OP [18], was observed (Fig. 4). However, neither hematopoietic lineage markers, such as CD45, CD11b, or Gr-1, nor endothelial lineage markers, such as CD34, Flk-1, or CD31, were detected. Interestingly, circulating CD45-negative MOPCs markedly expressed CXCR4 (Fig. 4), a receptor of the chemokine SDF-1 [19]. The SDF-1 chemokine is known to hold CXCR4-positive stem cells in the bone marrow niche [20–22] and to recruit those cells to peripheral tissues that express SDF-1 [23, 24].

SDF-1 Is Expressed by Vascular Cells and Osteoblasts in and Around the BMP-2 Implant

To determine whether the CXCR4 on the MOPCs played a functional role interacting with SDF-1 for migration to bone formation, we assessed SDF-1 expression in cells surrounding the BMP-2 implant. Immunofluorescence staining showed that CD31-positive and CD34-positive vascular endothelial cells adjacent to the BMP-2 collagen pellet highly expressed SDF-1 (Fig. 5A). The vasculatures expressing SDF-1 are likely to be arterioles, because they express smooth muscle actin at the periphery of the endothelial cells (Fig. 5A). Quantitative real-time PCR analysis also revealed marked elevation of SDF-1 expression in tissues containing BMP-2 pellets from day 1 to day 7 after implantation (Fig.

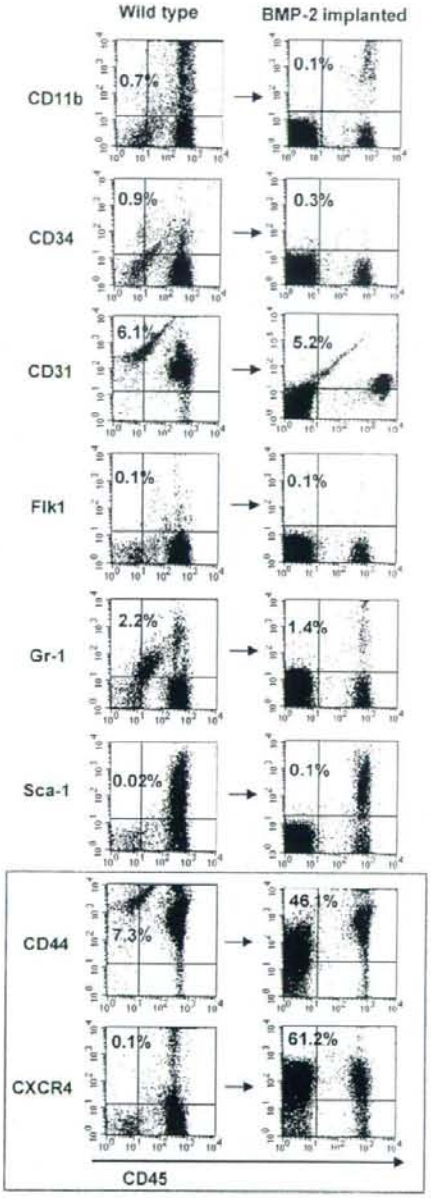

Figure 4. Flow cytometry analysis of marrow-derived osteoblast progenitor cells (MOPCs). Most of the peripheral blood mononuclear cells (PBMNCs) in wild-type mice (control) were CD45-positive, CD45-negative MOPCs were increased in PBMNCs of BMP-2 pellet-implanted mice on day 4. Endothelial lineage markers (CD34, CD31, and Flk1) and hematopoietic lineage markers (CD45, CD11b, and Gr-1) were not detected in the CD45-negative MOPCs in BMP-2-implanted mice. CD44 and CXCR4 were highly expressed in the CD45-negative MOPCs of BMP-2-implanted mice compared with the PBMNCs from wild-type mice. Abbreviation: BMP, bone morphogenetic protein.

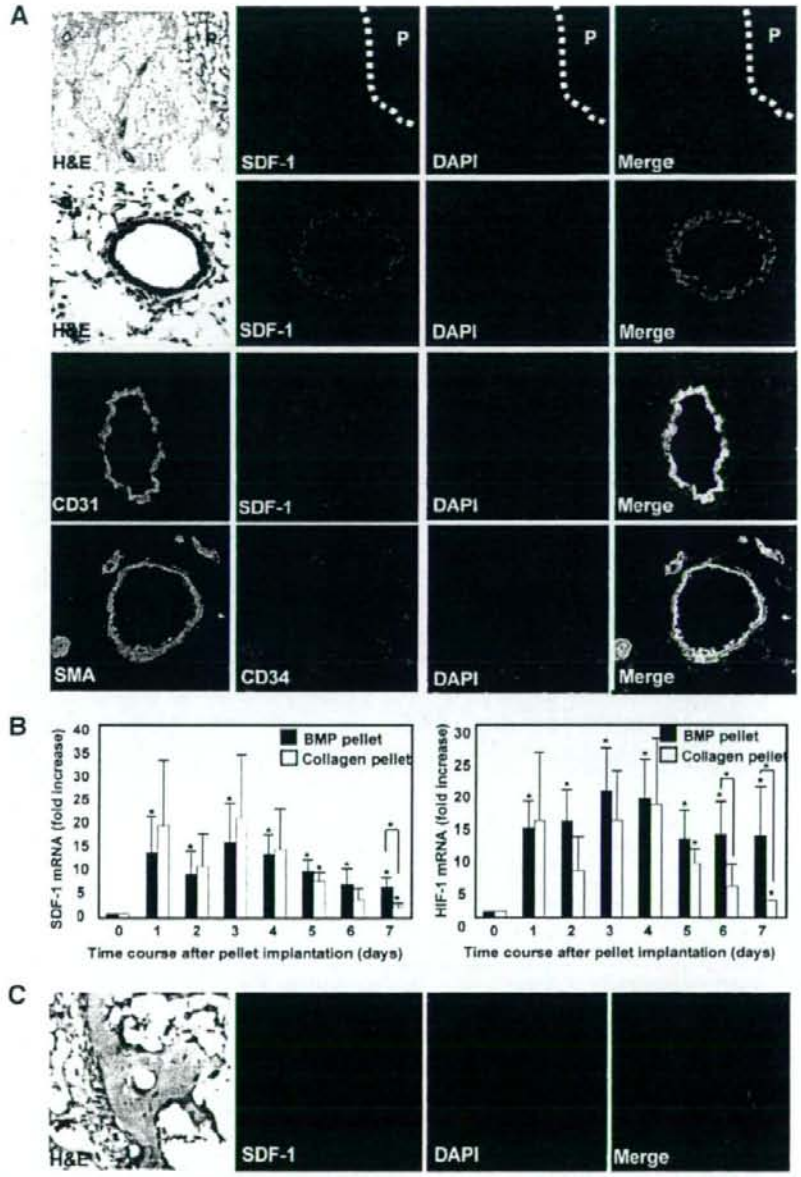

Figure 5. SDF-1 was expressed around the BMP-2 P. **(A):** Histologic H&E-staining and immunofluorescence staining showed that vessels around the BMP-2 P highly expressed SDF-1. Magnification, ×100 (first) and ×500 (second). Immunofluorescence staining of the serial sections of the SDF-1-positive section around the BMP-2 P showed that SDF-1 was expressed from the CD31-, CD34-, and SMA-positive vessel. Magnification, ×500. **(B):** The quantitative time-course analysis of SDF-1 and hypoxia inducible factor-1 (HIF-1) mRNA expression in the BMP-2 and collagen Ps revealed that SDF-1 and HIF-1 expression increased significantly in BMP-2 Ps compared with control tissue (day 0). *, $p < .01$. The high expression was significantly maintained on day 7 in BMP-2 Ps compared with those on day 7 in collagen Ps. *, $p < .01$. The fold increases of expression levels were normalized to those of control tissue (day 0). **(C):** The immunofluorescence staining of the BMP-2-induced ectopic bone on day 14 demonstrated osteoblasts lining the newly formed bone expressed SDF-1. Magnification, ×500. Abbreviations: BMP, bone morphogenetic protein; DAPI, 4′,6-diamidino-2-phenylindole; P, pellet; SDF, stromal cell-derived factor; SMA, smooth muscle actin.

5B). HIF-1, a transcriptional inducer of SDF-1 [23], was also highly elevated in and around the implanted pellets with or without BMP-2 in the early days, suggesting that nonspecific hypoxic conditions in the tissue induced the expression of HIF-1 and SDF-1 (Fig. 5B). After day 6, however, BMP-2 stimulation significantly and specifically sustained the expression of SDF-1 and HIF-1($p < .01$; Fig. 5B), suggesting that the continuous expression of SDF-1 in the regenerating

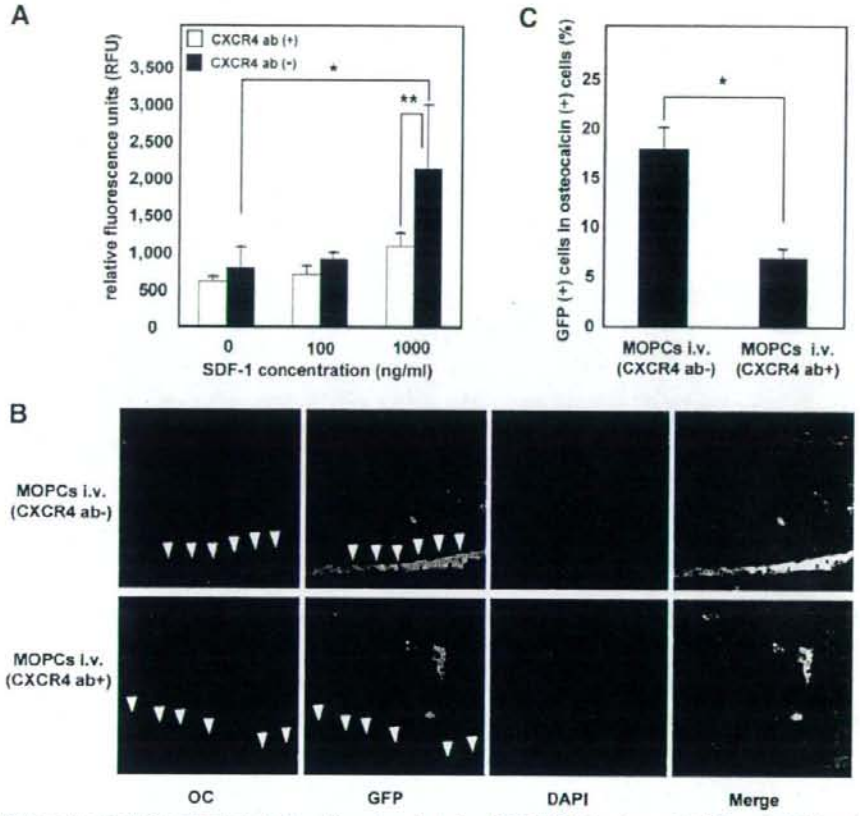

Figure 6. MOPCs in the circulation migrate to the bone formation site in the CXCR4/SDF-1 pathway. **(A):** Effect of SDF-1 on MOPCs in the circulation was checked in the Boyden chamber migration assay. The MOPC migration was stimulated by SDF-1. *, $p < .05$. The effect of SDF-1 was significantly decreased when the MOPCs were pretreated with CXCR4-blocking antibody. **, $p < .05$. The number of migrated cells was measured as RFU. **(B):** MOPCs from a BMP-2-implanted GFP transgenic mice were pretreated with or without the CXCR4-blocking antibody and were injected to a BMP-2-implanted nude mouse daily for 7 days. Immunofluorescence staining of ectopic bone from the nude mouse showed that injected GFP-positive MOPCs differentiated to OC-positive osteoblasts lining the newly formed trabecular bone. Fewer GFP- and OC-positive osteoblasts were found in sections of ectopic bone from a nude mouse injected daily for 7 days with the GFP transgenic MOPCs pretreated with the CXCR4-blocking antibody. Magnification, ×400. **(C):** Quantitative analysis of GFP-positive/OC-positive osteoblasts lining the trabecular bone showed that the MOPC migration was significantly blocked by blocking CXCR4. *, $p = .00019$. Abbreviations: RFU, relative fluorescence units; ab, antibody; DAPI, 4′,6-diamidino-2-phenylindole; GFP, green fluorescent protein; i.v., intravenous; MOPC, marrow-derived osteoblast progenitor cell; OC, osteocalcin; SDF, stromal cell-derived factor.

bone was due to BMP-2 stimulation. This speculation was confirmed by histologic analysis, which clearly indicated sustained SDF-1 expression in the regenerating osteoblasts aligning on the newly formed osseous tissues (Fig. 5C).

The CXCR4/SDF-1 System Plays an Important Role in the Recruitment of Circulating MOPCs to the Region of Ectopic Bone Formation

To examine the chemoattractant potential of SDF-1 for MOPCs in the peripheral blood, MOPCs in PBMNCs isolated from BMP-2 pellet-implanted mice were subjected to in vitro migration assays in a Boyden chamber. Approximately 2.5 times higher migration of the cells was observed in the lower chamber, which contained 1,000 ng/ml SDF-1, and this migration was clearly inhibited by incubating the cells with CXCR4-blocking antibody before the assay ($p < .05$; Fig. 6A). Furthermore, to check the in vivo chemotaxis of circulating MOPCs, we isolated MOPCs from PBMNCs daily from the BMP-2 pellet-implanted GFP-transgenic mice and injected the isolated MOPCs, with or without prior CXCR4-blocking antibody treatment, through the tail veins of BMP-2 pellet-implanted nude mice daily for 7 days. Two weeks later, histologic examination revealed that GFP-positive osteoblasts that originated from injected MOPCs made a significant contribution to ectopic bone formation, and the in vivo migration of the MOPCs to the implanted BMP-2 pellet was strongly inhibited by treatment of the isolated MOPCs with CXCR4-blocking antibody (Fig. 6B; supplemental online Fig. 3). The percentage of GFP-positive osteoblasts in osteocalcin-expressing osteoblasts was significantly decreased to 6.8% ± 0.9% in the ectopic bone by blocking CXCR4 on the MOPCs, whereas the percentage was 17.5% ± 2.3% in the ectopic bone from mice injected with MOPCs without CXCR4 blocking ($p = .00019$; Fig. 6C). These data strongly suggest that CXCR4 on circulating MOPCs functions as a receptor for SDF-1 to induce the migration of MOPCs to the region expressing SDF-1 in regenerating bone.

DISCUSSION

Circulating mesenchymal progenitor cells or osteoblast lineage cells have been shown to exist in various mammals, including humans and mice [6–8, 25, 26]. Those circulating osteoblast lineage cells were isolated from peripheral blood, expanded in culture, and inoculated to show their potency to become osteoblasts in vitro and in vivo. Major questions raised after those observations included where those circulating cells came from, where they went, and how they approached their destination in vivo.

Recently, we reported that marrow cells in intact bone are a major, if not exclusive, source of circulating OPCs under a BMP-2-induced ectopic bone-forming condition in mice, and these cells endogenously participate in the process of the ectopic bone formation [11]. In this study, a parabiotic pairing mouse model showed that ~50% of all osteoblasts were derived from MOPCs in the BMP-2-induced ectopic bone. Previous studies of fracture healing have shown that fracture stimulation induces BMP-2 expression in the surrounding tissues [27–29], suggesting that endogenously circulating MOPCs may also contribute to fracture healing, as well as to ectopic bone formation.

Circulating MOPCs seem to present as a small population without induction. Even after inducing stimulation, the increase of circulating MOPCs was time-limited and not maintained for more than few days. The peak of the MOPC induction in circulation oscillated between day 3 and day 7 after BMP-2 implantation, possibly because of the strength of signals generated by both BMP-2 and injury stimulation (data not shown). These findings may explain the previous difficulties in detecting circulating mesenchymal cells without expansion in culture [30, 31].

SDF-1 has been characterized as a potent CXC chemokine that is constitutively expressed in various cell types, including mesenchymal stem cells and osteoblasts, in bone marrow, and in dermal and synovial fibroblasts [22, 32, 33]. SDF-1 retains hematopoietic stem cells that express CXCR4, a receptor for SDF-1, in bone marrow [21, 22]. SDF-1 expressed in peripheral tissues under inflammatory conditions recruits circulating lymphocytes, monocytes, and other hematopoietic cells, except neutrophils, to the peripheral tissues via the CXCR4/SDF-1 system [34, 35]. A recent study showed that SDF-1 in mural cells around blood vessels functioned to entrap bone marrow-derived vascular endothelial progenitor cells, which express CXCR4, in circulation [36]. We demonstrated significant expression of CXCR4 on circulating MOPCs. A strong expression of SDF-1 was noted not in the circulating MOPCs (supplemental online Fig. 4) but in vascular endothelial cells and osteoblasts in the regions of the ectopic osteogenesis, suggesting that the CXCR4/SDF-1 system may play an important role in entrapping circulating MOPCs around the area of the bone formation, although factors besides SDF-1 may also contribute to the osteogenic processes with MOPCs recruitment. Further analysis showed that elevations of SDF-1 levels were accompanied by upregulation of HIF-1, a well-known transcriptional factor that upregulates SDF-1 expression. HIF-1 and SDF-1 induction were obtained by implantation of the collagen pellet without BMP-2 and probably resulted from the hypoxic tissue damage induced by surgical implantation of the pellet. The BMP-2 pellet, however, exhibited significantly prolonged expression of HIF-1 and SDF-1 at day 7 compared with the collagen pellet itself. This sustained expression of SDF-1 in the BMP-2-pellet was further confirmed in osteoblasts, as well as in vascular endothelial cells of the newly generating bone after day 7 (data not shown). Collectively, HIF-1-dependent initial expression of SDF-1 in arterioles around the BMP-2 pellet seemed to entrap circulating MOPCs, followed by BMP-2-dependent recruitment and differentiation of the trapped MOPCs to osteoblasts, which expressed SDF-1 and may have further enhanced bone formation by continuous recruitment of MOPCs to the osseous tissue in collaboration with the CXCR4/SDF-1 pathway. Previous studies [37, 38] also showed that the CXCR4/SDF-1 pathway plays a pivotal role in the migration of stem cells to regenerating tissues, suggesting that the hypoxic condition induced by tissue injury plays a role in the induction of SDF-1 expression at the initial stage of tissue regeneration.

Recent studies have indicated that CD44 binds to the ubiquitous matrix protein OP and serves as a receptor on CD44-expressing cells to bind to OP [18]. Osteopontin is known to be expressed in osteoblasts and secreted in the areas of the callus formation [39], suggesting that OP functions as the major ligand for CD44 on migrating osteoblast progenitor cells in the remodeling phase of fracture healing [40]. In this context, it is interesting to note that circulating MOPCs significantly expressed CD44 on the cell surface. Interaction between OP and CD44 on MOPCs may be important for the acceleration of bone formation in combination with the CXCR4/SDF-1 system and BMP stimulation.

Signals that trigger migration of the particular cell population from bone marrow to the circulation were not identified in this study. Vascular endothelial growth factor (VEGF) was previously shown to be sufficient for recruitment of marrow-derived vascular endothelial progenitor cells into the circulation [36]. We also observed elevation of VEGF levels in muscular tissue around the implanted collagen pellet (data not shown). This observation may suggest that VEGF contributes to angiogenesis in the area of bone regeneration, although further evidence must be obtained to support this conclusion. Implantation of the collagen pellet itself induced a significant number of MOPCs in the circulation, suggesting that surgical injury may induce production of MOPC-recruiting signals, probably because of hypoxic stress in injured tissue, as previously reported [41]. BMP-2-pellet implantation, however, induced a relatively higher increase in MOPCs in the circulation compared with empty collagen pellets. In addition, subcutaneous injection of BMP-2 without extensive tissue damage could induce ~20% of CD45-negative cells in circulation (data not shown), suggesting that both BMP-2 and tissue injury contribute to the mobilization of MOPCs in circulation. A lack of detectable expression of bone morphogenetic protein receptor II (BMPR-II) on the MOPCs in the circulation (supplemental online Fig. 5) suggests that BMP-2 does not participate in MOPC mobilization but that other factors induced by BMP-2 may. This hypothesis may be supported by our observation that there were no significant changes in the concentration of BMP-2 in serum between wild-type nontreated mice and BMP-2 pellet-implanted mice (supplemental online Fig. 5). Furthermore, we could establish a C57BL/6 mouse bone marrow-derived stromal cell line, which had been shown to be negative for BMPR-II but maintained the capability to differentiate to mature mineralizing osteoblasts when cultured in osteogenic medium (S. Otsuru et al., unpublished data), suggesting that BMPR-II expression may not be essential to maintain osteogenic features in the initial undifferentiated condition of the MOPCs.

The importance of providing additional OPCs to the site of bone formation has been shown by a number of previous studies [42–47]. Identification of signals that induce migration of MOPCs in the circulation may have clinical applications in the future, as the ability to increase MOPCs in the circulation may help patients with intractable bone fractures by inducing further accumulation of MOPCs to the fractured lesion. Robust induction of circulating MOPCs may also enable us to easily isolate these cells by simple blood sampling, providing the possibility

to develop novel cell-based regenerative therapies for intractable bone fractures and possibly for other damaged tissues. Because current procedures to isolate cells directly from bone marrow are invasive, the easy isolation of MOPCs from peripheral blood has advantages in terms of safety, repeatability, and acceptability. Genetic manipulation of isolated MOPCs may also have possible applications in the treatment of genetic disorders such as osteogenesis imperfecta [48, 49].

The potency of circulating MOPCs as stem cells is another issue to be addressed in future studies. Because Sca-1 is an established marker of both mesenchymal and hematopoietic stem cells, MOPCs with low levels of Sca-1 expression seem to have different features compared with stem cells in bone marrow [50, 51]. Demonstration of efficient differentiation activities of MOPCs, in addition to osteoblastic lineage, may illustrate the additional importance of these cells in tissue regeneration.

CONCLUSION

We report here the crucial role of the CXCR4/SDF-1 pathway in the bone formation involving circulating MOPCs. The mobilized MOPCs that expressed CXCR4 were recruited to the bone-forming site by SDF-1 expressed in vascular endothelial cells and the de novo osteoblasts of the region. These data may provide perspective on the use of circulating MOPCs to accelerate bone regeneration in the future.

ACKNOWLEDGMENTS

This work was supported by the Northern Osaka (Saito) Biomedical Knowledge-Based Cluster Creation Project and a Grant-in-Aid from the Ministry of Education, Culture, Sports, Science and Technology of Japan.

DISCLOSURE OF POTENTIAL CONFLICTS OF INTEREST

The authors indicate no potential conflicts of interest.

REFERENCES

1 Jiang Y, Jahagirdar BN, Reinhardt RL et al. Pluripotency of mesenchymal stem cells derived from adult marrow. Nature 2002;418:41–49.
2 Pittenger MF, Mackay AM, Beck SC et al. Multilineage potential of adult human mesenchymal stem cells. Science 1999;284:143–147.
3 Prockop DJ. Marrow stromal cells as stem cells for nonhematopoietic tissues. Science 1997;276:71–74.
4 Minguell JJ, Erices A, Conget P. Mesenchymal stem cells. Exp Biol Med (Maywood) 2001;226:507–520.
5 Pereira RF, Halford KW, O'Hara MD et al. Cultured adherent cells from marrow can serve as long-lasting precursor cells for bone, cartilage, and lung in irradiated mice. Proc Natl Acad Sci U S A 1995;92:4857–4861.
6 Eghbali-Fatourechi GZ, Lamsam J, Fraser D et al. Circulating osteoblast-lineage cells in humans. N Engl J Med 2005;352:1959–1966.
7 Kuznetsov SA, Mankani MH, Gronthos S et al. Circulating skeletal stem cells. J Cell Biol 2001;153:1133–1140.
8 Wan C, He Q, Li G. Allogenic peripheral blood derived mesenchymal stem cells (MSCs) enhance bone regeneration in rabbit ulna critical-sized bone defect model. J Orthop Res 2006;24:610–618.
9 Wozney JM, Rosen V, Celeste AJ et al. Novel regulators of bone formation: Molecular clones and activities. Science 1988;242:1528–1534.
10 Takaoka K, Nakahara H, Yoshikawa H et al. Ectopic bone induction on and in porous hydroxyapatite combined with collagen and bone morphogenetic protein. Clin Orthop Relat Res 1988:250–254.
11 Otsuru S, Tamai K, Yamazaki T et al. Bone marrow-derived osteoblast progenitor cells in circulating blood contribute to ectopic bone formation in mice. Biochem Biophys Res Commun 2007;354:453–458.
12 Okabe M, Ikawa M, Kominami K et al. 'Green mice' as a source of ubiquitous green cells. FEBS Lett 1997;407:313–319.
13 Wright DE, Wagers AJ, Gulati AP et al. Physiological migration of hematopoietic stem and progenitor cells. Science 2001;294:1933–1936.
14 Wakabayashi S, Tsutsumimoto T, Kawasaki S et al. Involvement of phosphodiesterase isozymes in osteoblastic differentiation. J Bone Miner Res 2002;17:249–256.
15 Tamai N, Myoui A, Tomita T et al. Novel hydroxyapatite ceramics with an interconnective porous structure exhibit superior osteoconduction in vivo. J Biomed Mater Res 2002;59:110–117.
16 Nishikawa M, Myoui A, Ohgushi H et al. Bone tissue engineering using novel interconnected porous hydroxyapatite ceramics combined with marrow mesenchymal cells: Quantitative and three-dimensional image analysis. Cell Transplant 2004;13:367–376.
17 Nishikawa M, Ohgushi H, Tamai N et al. The effect of simulated microgravity by three-dimensional clinostat on bone tissue engineering. Cell Transplant 2005;14:829–835.
18 Weber GF, Ashkar S, Glimcher MJ et al. Receptor-ligand interaction between CD44 and osteopontin (Eta-1). Science 1996;271:509–512.
19 Bleul CC, Farzan M, Choe H et al. The lymphocyte chemoattractant SDF-1 is a ligand for LESTR/fusin and blocks HIV-1 entry. Nature 1996;382:829–833.
20 Dar A, Goichberg P, Shinder V et al. Chemokine receptor CXCR4-dependent internalization and resecretion of functional chemokine SDF-1 by bone marrow endothelial and stromal cells. Nat Immunol 2005;6:1038–1046.
21 Ma Q, Jones D, Springer TA. The chemokine receptor CXCR4 is required for the retention of B lineage and granulocytic precursors within the bone marrow microenvironment. Immunity 1999;10:463–471.
22 Nagasawa T, Hirota S, Tachibana K et al. Defects of B-cell lymphopoiesis and bone-marrow myelopoiesis in mice lacking the CXC chemokine PBSF/SDF-1. Nature 1996;382:635–638.
23 Ceradini DJ, Kulkarni AR, Callaghan MJ et al. Progenitor cell trafficking is regulated by hypoxic gradients through HIF-1 induction of SDF-1. Nat Med 2004;10:858–864.
24 Ratajczak MZ, Majka M, Kucia M et al. Expression of functional CXCR4 by muscle satellite cells and secretion of SDF-1 by muscle-derived fibroblasts is associated with the presence of both muscle progenitors in bone marrow and hematopoietic stem/progenitor cells in muscles. STEM CELLS 2003;21:363–371.
25 Fernandez M, Simon V, Herrera G et al. Detection of stromal cells in peripheral blood progenitor cell collections from breast cancer patients. Bone Marrow Transplant 1997;20:265–271.
26 Roufosse CA, Direkze NC, Otto WR et al. Circulating mesenchymal stem cells. Int J Biochem Cell Biol 2004;36:585–597.
27 Bostrom MP. Expression of bone morphogenetic proteins in fracture healing. Clin Orthop Relat Res 1998:S116–S123.
28 Bostrom MP, Lane JM, Berberian WS et al. Immunolocalization and expression of bone morphogenetic proteins 2 and 4 in fracture healing. J Orthop Res 1995;13:357–367.
29 Ishidou Y, Kitajima I, Obama H et al. Enhanced expression of type I receptors for bone morphogenetic proteins during bone formation. J Bone Miner Res 1995;10:1651–1659.
30 Lazarus HM, Haynesworth SE, Gerson SL et al. Human bone marrow-derived mesenchymal (stromal) progenitor cells (MPCs) cannot be recovered from peripheral blood progenitor cell collections. J Hematother 1997;6:447–455.
31 Wexler SA, Donaldson C, Denning-Kendall P et al. Adult bone marrow is a rich source of human mesenchymal 'stem' cells but umbilical cord and mobilized adult blood are not. Br J Haematol 2003;121:368–374.
32 Nagasawa T, Nakajima T, Tachibana K et al. Molecular cloning and characterization of a murine pre-B-cell growth-stimulating factor/stromal cell-derived factor 1 receptor, a murine homolog of the human immunodeficiency virus 1 entry coreceptor fusin. Proc Natl Acad Sci U S A 1996;93:14726–14729.
33 Zvaifler NJ, Marinova-Mutafchieva L, Adams G et al. Mesenchymal precursor cells in the blood of normal individuals. Arthritis Res 2000;2:477–488.
34 Aiuti A, Webb IJ, Bleul C et al. The chemokine SDF-1 is a chemoattractant for human CD34+ hematopoietic progenitor cells and provides a new mechanism to explain the mobilization of CD34+ progenitors to peripheral blood. J Exp Med 1997;185:111–120.

35 Bleul CC, Fuhlbrigge RC, Casasnovas JM et al. A highly efficacious lymphocyte chemoattractant, stromal cell-derived factor 1 (SDF-1). J Exp Med 1996;184:1101–1109.
36 Grunewald M, Avraham I, Dor Y et al. VEGF-induced adult neovascularization: Recruitment, retention, and role of accessory cells. Cell 2006; 124:175–189.
37 Imitola J, Raddassi K, Park KI et al. Directed migration of neural stem cells to sites of CNS injury by the stromal cell-derived factor 1alpha/CXC chemokine receptor 4 pathway. Proc Natl Acad Sci U S A 2004; 101:18117–18122.
38 Ji JF, He BP, Dheen ST et al. Interactions of chemokines and chemokine receptors mediate the migration of mesenchymal stem cells to the impaired site in the brain after hypoglossal nerve injury. STEM CELLS 2004;22:415–427.
39 Hirakawa K, Hirota S, Ikeda T et al. Localization of the mRNA for bone matrix proteins during fracture healing as determined by in situ hybridization. J Bone Miner Res 1994;9:1551–1557.
40 Yamazaki M, Nakajima F, Ogasawara A et al. Spatial and temporal distribution of CD44 and osteopontin in fracture callus. J Bone Joint Surg Br 1999;81:508–515.
41 Rochefort GY, Delorme B, Lopez A et al. Multipotential mesenchymal stem cells are mobilized into peripheral blood by hypoxia. STEM CELLS 2006;24:2202–2208.
42 Curylo LJ, Johnstone B, Petersilge CA et al. Augmentation of spinal arthrodesis with autologous bone marrow in a rabbit posterolateral spine fusion model. Spine 1999;24:434–438; discussion 438–439.
43 Grundel RE, Chapman MW, Yee T et al. Autogeneic bone marrow and porous biphasic calcium phosphate ceramic for segmental bone defects in the canine ulna. Clin Orthop Relat Res 1991:244–258.
44 Lindholm TS, Nilsson OS, Lindholm TC. Extraskeletal and intraskeletal new bone formation induced by demineralized bone matrix combined with bone marrow cells. Clin Orthop Relat Res 1982:251–255.
45 Lindholm TS, Ragni P, Lindholm TC. Response of bone marrow stroma cells to demineralized cortical bone matrix in experimental spinal fusion in rabbits. Clin Orthop Relat Res 1988:296–302.
46 Takagi K, Urist MR. The role of bone marrow in bone morphogenetic protein-induced repair of femoral massive diaphyseal defects. Clin Orthop Relat Res 1982:224–231.
47 Werntz JR, Lane JM, Burstein AH et al. Qualitative and quantitative analysis of orthotopic bone regeneration by marrow. J Orthop Res 1996;14:85–93.
48 Chamberlain JR, Schwarze U, Wang PR et al. Gene targeting in stem cells from individuals with osteogenesis imperfecta. Science 2004;303: 1198–1201.
49 Horwitz EM, Prockop DJ, Fitzpatrick LA et al. Transplantability and therapeutic effects of bone marrow-derived mesenchymal cells in children with osteogenesis imperfecta. Nat Med 1999;5:309–313.
50 Meirelles LS, Nardi NB. Murine marrow-derived mesenchymal stem cell: Isolation, in vitro expression, and characterization. Br J Haematol 2003;123:702–711.
51 Baddoo M, Hill K, Wilkinson R et al. Characterization of mesenchymal stem cells isolated from murine bone marrow by negative selection. J Cell Biochem 2003;89:1235–1249.

See www.StemCells.com for supplemental material available online.

The FASEB Journal • Research Communication

Angiotensin II accelerates osteoporosis by activating osteoclasts

Hideo Shimizu,*,†,[1] Hironori Nakagami,‡,[1] Mariana Kiomy Osako,* Rie Hanayama,* Yasuo Kunugiza,§ Takuji Kizawa,§ Tetsuya Tomita,§ Hideki Yoshikawa,§ Toshio Ogihara,† and Ryuichi Morishita*,[2]

*Division of Clinical Gene Therapy, †Department of Geriatric Medicine, ‡Division of Gene Therapy Science, and §Department of Orthopedic Surgery, Osaka University Graduate School of Medicine, Osaka, Japan

ABSTRACT **Recent clinical studies suggest that several antihypertensive drugs, especially angiotensin-converting enzyme inhibitors, reduced bone fractures. To clarify the relationship between hypertension and osteoporosis, we focused on the role of angiotensin II (Ang II) on bone metabolism. In bone marrow-derived mononuclear cells, Ang II (1×10^{-6} M) significantly increased tartrate-resistant acid phosphatase (TRAP) -positive multinuclear osteoclasts. Of importance, Ang II significantly induced the expression of receptor activator of NF-κB ligand (RANKL) in osteoblasts, leading to the activation of osteoclasts, whereas these effects were completely blocked by an Ang II type 1 receptor blockade (olmesartan) and mitogen-activated protein kinase kinase inhibitors. In a rat ovariectomy model of estrogen deficiency, administration of Ang II (200 ng/kg/min) accelerated the increase in TRAP activity, accompanied by a significant decrease in bone density and an increase in urinary deoxypyridinoline. In hypertensive rats, treatment with olmesartan attenuated the ovariectomy-induced decrease in bone density and increase in TRAP activity and urinary deoxypyridinoline. Furthermore, in wild-type mice ovariectomy with five-sixths nephrectomy decreased bone volume by microcomputed tomography, whereas these change was not detect in Ang II type 1a receptor-deficient mice. Overall, Ang II accelerates osteoporosis by activating osteoclasts *via* RANKL induction. Blockade of Ang II might become a novel therapeutic approach to prevent osteoporosis in hypertensive patients.—Shimizu, H., Nakagami, H., Osako, M. K., Hanayama, R., Kunugiza, Y., Kizawa, T., Tomita, T., Yoshikawa, H., Ogihara, T., Morishita, R. Angiotensin II accelerates osteoporosis by activating osteoclasts. *FASEB J.* 22, 2465–2475 (2008)**

Key Words: hypertension · renin-angiotensin system · RANKL · ARB · TRAP activity

HYPERTENSION AND OSTEOPOROSIS are two common diseases in the elderly population, which are caused by the interaction of genetic and environmental factors. As 50% of the hypertensive population comprises postmenopausal women at high risk of osteoporosis, hypertension represents a considerable health problem in this population. Animal and epidemiological evidence suggests that high blood pressure is associated with abnormalities of calcium metabolism, leading to an increase in calcium loss, secondary activation of the parathyroid gland, and increased movement of calcium from bone, thereby increasing the risk of osteoporosis (1, 2). Indeed, clinical studies have shown that antihypertensive drugs such as thiazides decrease the risk of hip fracture by reducing renal calcium excretion (3, 4). However, other antihypertensive drugs [β-blockers and angiotensin-converting enzyme (ACE) inhibitors] are also associated with a reduced risk of fractures (5), whereas calcium antagonists did not reduce the risk (5). Recent clinical studies also support the benefit of ACE inhibitors to reduce risk of fractures or improve bone metabolism (6, 7). These data suggest that the renin-angiotensin system might be involved in bone metabolism.

Because the vasculature plays an important role in bone remodeling, the effect of the renin-angiotensin system on bone metabolism may be partially related to the regulation of blood flow. However, there is no report documenting a direct relation of the renin-angiotensin system with bone metabolism. Although previous reports showed that the receptor for Ang II is expressed in osteoblasts and osteoclasts, the effects of Ang II are controversial (8, 9). Therefore, in this study, we examined whether the renin-angiotensin system is directly involved in bone metabolism, focusing on osteoclast activation.

MATERIALS AND METHODS

Cell culture

Bone marrow cells were obtained from 3-day-old neonatal white rabbits as described previously (10). Briefly, rabbit bone

[1] These authors contributed equally to this work.

[2] Correspondence: Division of Clinical Gene Therapy, Osaka University Graduate School of Medicine, 2-2 Yamadaoka, Suita, Osaka 565-0871, Japan. E-mail: morishit@cgt.med.osaka-u.ac.jp

doi: 10.1096/fj.07-098954

marrow cells were flushed out from the femurs and tibiae, collected into tubes, and washed twice with PBS. The mononuclear cell-rich fraction was separated from marrow cells by density gradient centrifugation with Ficoll and cultured (1×10^5 cells/well of 24-well plate) in α-minimal essential medium (α-MEM) containing 10% FBS.

Osteoclast differentiation was also examined using a rat osteoclast culture system obtained from Hokudo Co. Ltd. (Sapporo, Japan). Rat osteoclast precursor cells seeded in a 24-well plate were incubated with macrophage colony-stimulating factor (M-CSF) (10 ng/ml) and receptor activator of NF-κB ligand (RANKL; also called OPGL, TRANCE, and ODF) (10 ng/ml) -containing medium or Ang II (1×10^{-6}, 1×10^{-7}, or 1×10^{-8} M) to examine the differentiation of osteoclasts. Human osteoblasts or osteoclast precursors were obtained from Cell Applications (San Diego, CA, USA) or Lonza (Walkersville, MD, USA), respectively.

Tartrate-resistant acid phosphatase (TRAP) staining

After treatment with 1,25-dihydroxyvitamin D_3 (vitamin D_3) (1×10^{-8} M) or Ang II (1×10^{-8}, 1×10^{-7}, or 1×10^{-6} M), mononuclear cells were fixed with 4.0% paraformaldehyde in PBS for 10 min at room temperature before being stained for TRAP. Rat osteoclasts were treated similarly after treatment with M-CSF and RANKL or Ang II (1×10^{-6}, 1×10^{-7}, or 1×10^{-8} M). Enzyme histochemical staining for TRAP and Hoechst 33526 nuclear staining were performed as reported previously (11).

Real-time reverse transcription (RT) -polymerase chain reaction (PCR)

Human RANKL, receptor activator of NF-κB (RANK), and osteoprotegerin (OPG) expressions were measured by real-time RT-PCR. Total RNA of cells or tissue samples was extracted using an RNeasy Mini Kit (Qiagen, Valencia, CA, USA) or Isogen (Nippon Gene, Toyama, Japan). cDNA was synthesized using the Thermo Script RT-PCR System (Invitrogen, Carlsbad, CA, USA). Relative gene copy numbers of RANKL, OPG, and glyceraldehyde-3-phosphate dehydrogenase (GAPDH) were quantified by real-time RT-PCR using TaqMan Gene Expression Assays (human RANKL: Hs00243522, human OPG: Hs00900360, human RANK: Hs00921375, and human GAPDH: Hs99999905; Applied Biosystems, Foster City, CA, USA). The absolute number of gene copies was normalized using GAPDH and standardized by a sample standard curve.

Western blotting

Western blotting was performed for analysis of extracellular signal-regulated kinase (ERK), p38 mitogen-activated protein kinase (MAPK), and Akt expression using a phospho-specific antibody as described previously (12). After treatment, cells were extracted with lysis buffer (50 mM Tris-Cl, 2.5 mM EGTA, 1 mM EDTA, 10 mM NaF, 1% Triton X-100, 1 mM PMSF, and 2 mM Na_3VO_4). Samples containing 20 μg of protein were separated on 10% sodium dodecyl sulfate (SDS) -polyacrylamide gels, transferred to nitrocellulose membranes (Hybond ECL; Amersham Biosciences Corp., Piscataway, NJ, USA), and incubated with a polyclonal antibody against phospho-specific or total ERK, phospho-specific or total p38 MAPK, and phospho-specific or total Akt (polyclonal rabbit IgG, 1:1000; Cell Signaling Technology Inc., Danvers, MA, USA) at 4°C overnight. The membranes were then washed and incubated with a 1:5000 dilution of anti-rabbit IgG horseradish peroxidase-conjugated antibody (Amersham Biosciences Corp.). Bound antibodies were detected by enhanced chemiluminescence (Amersham Biosciences Corp.) and Hyperfilm-MP (Amersham Biosciences Corp.).

Inhibition of ERK, Akt, and p38 MAPK

To examine the effect of ERK, p38 MAPK, and Akt in the regulation of RANKL expression, human osteoblasts were pretreated (30 min) by the inhibitors of MEK (U0126, 50 μM; Calbiochem, San Diego, CA, USA), p38 MAPK (SB203580, 10 μM; Cell Signaling Technology Inc.), and phosphatidylinositol 3-kinase (PI3K) (LY294002, 50 μM or wortmannin, 100 nM; Calbiochem) in preparation for assays.

Quantification of RANKL and OPG protein

Human osteoblasts seeded in a 24-well plate were incubated with vitamin D_3 (1×10^{-8} M) or Ang II (1×10^{-6} M) with pretreatment (30 min) with olmesartan (1×10^{-5} M) or PD123329 (1×10^{-5} M) for 48 h. Soluble RANKL and OPG in the conditioned medium were measured according to the manufacturer's instructions (Biomedica Medizinprodukte, Vienna, Austria). Western blotting was also performed for analysis of RANKL expression using an anti-human RANKL antibody (polyclonal goat IgG, 1:1000; R&D Systems, Minneapolis, MN, USA) and an anti-β-actin (monoclonal mouse IgG, 1:3000; Sigma-Aldrich Corp., St. Louis, MO, USA).

RNA Interference and oligodeoxynucleotides

The small interfering (si) RNA for human RANK or scramble siRNA was designed using the siSNIPER system (Genomidea, Inc., Ibaraki, Japan, and Mitsubishi Space Software Co., Ltd., Amagasaki, Japan). The sequence of human RANK (sense) was 5′-GUACCAGUGAGAAGCAUUATT-3′ and the sequence of scramble siRNA (sense) was 5′-CGAGACCCGUUCACAUUGATT-3′. The siRNA oligonucleotides were transfected into human osteoclast precursors using a Human Macrophage Nucleofector Kit (Amaxa Biosystems, Cologne, Germany) according to the manufacturer's instructions (13).

Osteoclast formation assay

An osteoclast formation assay was performed using cocultures of human osteoblasts and osteoclast precursors as described previously (14). Human osteoblasts seeded in a 24-well plate were incubated with vitamin D_3 (1×10^{-8} M) or Ang II (1×10^{-6} M) with pretreatment (30 min) with olmesartan (1×10^{-5} M) or PD123329 (1×10^{-5} M) for 48 h and fixed in PBS containing 1% paraformaldehyde for 8 min at room temperature. Human osteoclast precursors were also cultured for 6 days on the fixed cells in α-MEM containing 10% FCS and 10 ng/ml of human M-CSF in a 24-well plate. After treatment, the cells were subjected to TRAP staining and nuclear staining as described above.

Rat ovariectomy osteoporosis model

Female adult Wister rats (10 wk old) were purchased from SLC Japan (Shizuoka, Japan). After the rats were anesthetized with intraperitoneal ketamine (80 mg/kg) and xylazine (10 mg/kg), bilateral ovariectomy or sham operation was performed, and an osmotic minipump (Alzet model 2004; Alza, Palo Alto, CA) containing a subpresser dose of Ang II (200 ng/kg/min) or saline was implanted (15). Female adult spontaneously hypertensive rats (SHRs) or Wistar-Kyoto rats (WKYs) (10 wk old) were also purchased from SLC Japan, and

bilateral ovariectomy or sham operation was performed. In some groups of rats, an osmotic minipump containing olmesartan (0.5, 1, or 3 mg/kg/day) was implanted, and in another group of rats hydralazine (10 mg/kg/day) was administered with drinking water. The body weights of these rats were recorded for 4 wk. At 4 wk after operation, systolic blood pressure was then measured using the tail-cuff method (BP-98A; Softron Beijing Incorporated, Beijing, China), and rats were deeply anesthetized and sacrificed to collect femurs, tibiae, and blood for biochemical analysis. Both TRAP and alkaline phosphatase (ALP) activity were measured to evaluate the total balance of osteoclast and osteoblast activity in the process of osteoporosis. The proximal tibia and distal femur were excised and homogenized in 10 mM triethanolamine buffer (pH 7.5) for TRAP activity and diethanolamine buffer (pH 9.8) for ALP activity. Supernatants were subjected to measurement of TRAP activity as described previously (11). For ALP activity, supernatants were incubated with *p*-nitrophenylphosphate as a substrate for 30 min at 25°C, and absorbance was measured at 405 nm. The urinary deoxypyridinoline level was measured by enzyme immunoassay (Metra Biosystems, Mountain View, CA, USA) on day 28 of the experiments.

Dual energy X-ray absorptiometry (DEXA) and microcomputed tomography

Bone density measurements were performed by DEXA bone densitometry (GE-Lunar DPX-IQ; Madison, WI, USA). High- and low-beam energies for all scans were 80 and 35 kV, respectively, at 0.5 mA as described previously (16). Bone mineral density was obtained in g/cm^2.

Bone microarchitecture was analyzed by using cone beam microcomputed tomography (X-ray computed tomography system, SMX-100CT-SV; Shimazu, Osaka, Japan) and software (TRI/3D-BON; RATOC System Engineering Co. Ltd., Tokyo, Japan), which serves as a valuable tool for evaluating both antiresorptive and anabolic agents in ovariectomized (OVX) mice (17). Briefly, the proximal tibia metaphysis was scanned at the region of 0.65–2.35 mm under the growth plate. A total of 135 consecutive tomographic slices were obtained with a slice thickness of 12.8 μm at 8 μm resolution. After scanning, three-dimensional microstructual image data were reconstructed and structural indices were calculated using the three-dimensional trabecular bone analysis software TRI/3D-BON as described previously (18). The gray-scale images were segmented using a median filter to remove noise and a fixed threshold to extract the mineralized bone phase. Subsequently, the isolated small particles in the marrow space and the isolated small holes in the bone were removed using a cluster-labeling algorithm. The trabecular bone was then separated and analyzed for structural indices. Bone volume was calculated using tetrahedrons corresponding to the enclosed volume of the triangulated surface. Total tissue volume was the volume of the entire scanned sample. Trabecular bone volume fraction was calculated from these values. Trabecular thickness and space were estimated as described previously (19).

Five-sixths nephrectomy and OVX model

Angiotensin II type 1A receptor-deficient (AT_{1A} KO) mice (20) (n=10; The Jackson Laboratory, Bar Harbor, ME, USA) and wild-type mice (n=10), 8 wk old, from the same genetic background (C57BL/6 mice) (Oriental Bioservice Co., Ltd., Kyoto, Japan) were used in the present study. Adult female mice, fed standard rat chow with free access to water, were subjected to subtotal renal ablation (21). Infarction of the left kidney was produced by ligation of two segmental renal arteries, and 2 weeks later, right nephrectomy and ovariectomy were performed. After ablation, systolic blood pressure was measured by the tail-cuff technique.

Statistical analysis

All values are expressed as means ± SE. Analysis of variance with subsequent Bonferroni/Dunnet's test was used to determine the significance of differences in multiple comparisons. Values of $P < 0.05$ were considered to be statistically significant.

RESULTS

Effect of Ang II on osteoclast differentiation

To clarify the direct effects of Ang II on osteoporosis, we initially focused on the differentiation of osteoclasts in two different cell culture systems. In rabbit bone marrow-derived mononuclear cells, which may include both osteoblasts and osteoclasts, treatment with Ang II (1×10^{-6} M) and with vitamin D_3 (1×10^{-8} M) induced osteoclast differentiation as assessed by Hoechst 33258 nuclear staining and TRAP staining. These effects were significantly abolished by cotreatment with an Ang II type 1 receptor blocker, olmesartan, but not with an Ang II type 2 receptor blocker, PD123329 (**Fig. 1*A***). To address the target of Ang II in osteoclast differentiation, we used a rat osteoclast culture system that was dependent on treatment with recombinant RANKL and M-CSF without coculture of osteoblasts. Unexpectedly, treatment with Ang II and with 1,25-dihydroxyvitamin D_3 (vitamin D_3) did not increase TRAP-positive multinuclear cells (Fig. 1*B*), although the treatment with RANKL and M-CSF increased TRAP-positive multinuclear cells. These results suggest that the osteoclast itself is not the direct target of Ang II in the process of osteoclast differentiation.

Therefore, we examined the effect of Ang II on osteoblasts. Cell viability (assessed by the MTS assay) was not significantly changed by treatment with Ang II (1×10^{-6} M) (data not shown). However, stimulation with Ang II (1×10^{-6} M) led to an increase in RANKL mRNA expression by 8-fold and in OPG (decoy receptor for RANKL) by 3-fold as quantified by real-time PCR (**Fig. 2*A***). We confirmed that soluble RANKL protein was up-regulated by Ang II (1×10^{-6} M), as shown in Fig. 2*B*, consistent with the results of Western blotting (Fig. 2*C*). Furthermore, we also confirmed that OPG protein was up-regulated by Ang II (1×10^{-6} M), as shown in Fig. 2*D*. These effects of Ang II in osteoblasts were significantly abolished by pretreatment with an Ang II type 1 receptor blocker, olmesartan, but not by an Ang II type 2 receptor blocker, PD123329. These results suggest that Ang II directly induced RANKL expression in osteoblasts through the activation of the Ang II type 1 receptor, leading to osteoclast activation.

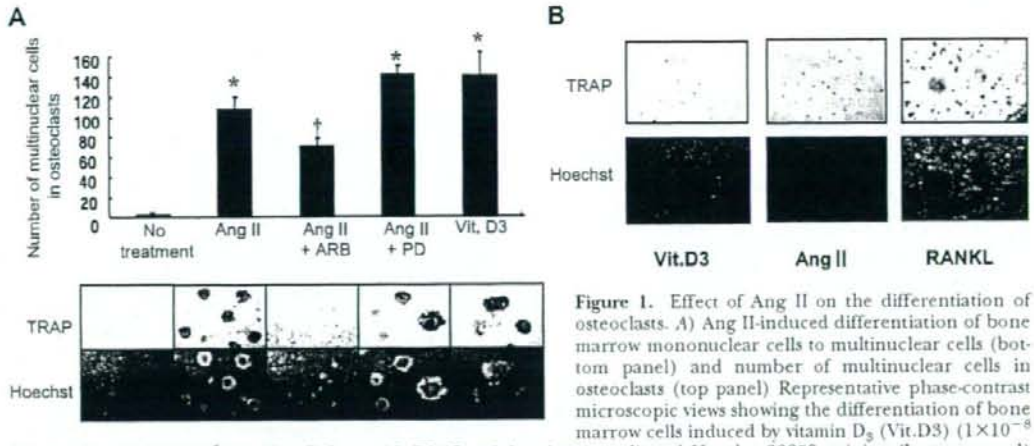

Figure 1. Effect of Ang II on the differentiation of osteoclasts. *A*) Ang II-induced differentiation of bone marrow mononuclear cells to multinuclear cells (bottom panel) and number of multinuclear cells in osteoclasts (top panel) Representative phase-contrast microscopic views showing the differentiation of bone marrow cells induced by vitamin D_3 (Vit.D3) (1×10^{-8} M) and Ang II (1×10^{-6} M) after 7 days, with TRAP staining (top panel) and Hoechst 33258 staining (bottom panel) (×40). ARB, treatment with an Ang II type 1 receptor blocker, olmesartan (1×10^{-5} M); PD, treatment with an Ang II type 2 receptor blocker, PD123329 (1×10^{-5} M). *B*) Effect of Ang II on TRAP activity in RANKL- and M-CSF-dependent rat osteoclasts. Representative phase-contrast microscopic views showing the differentiation of rat preosteoclast induced by vitamin D3 (1×10^{-8} M), Ang II (1×10^{-6} M), and RANKL (10 ng/ml RANKL+10 ng/ml M-CSF) after 7 days, with TRAP staining (top panel) and Hoechst 33258 staining (bottom panel) (×40).

We clarified the cellular signaling of Ang II, leading to up-regulation of RANKL in osteoblasts. Treatment with Ang II rapidly increased phosphorylation of ERK, p38 MAPK, and Akt, whereas this activation was blocked by pretreatment with an angiotensin receptor blocker but not with PD123329 (Fig. 2*E*). Pretreatment with an angiotensin receptor blocker also blocked the up-regulation of Ang II-induced RANKL expression. Similarly, pretreatment with U0126 (MEK inhibitor) attenuated Ang II-induced up-regulation of RANKL protein, whereas SB203580 (p38 MAPK inhibitor) and wortmannin (PI3K inhibitor) did not (Fig. 2*F*). To confirm the function of Ang II-induced up-regulation of RANKL protein, we examined the differentiation of osteoclasts using a coculture system with osteoblasts and osteoclast precursors. Treatment with Ang II and with vitamin D_3 induced the number of TRAP-positive multinuclear cells. Pretreatment with an angiotensin receptor blocker or U0126 attenuated the Ang II-induced increase of the number of TRAP-positive multinuclear cells, whereas SB203580 and wortmannin did not (Fig. 2*G*). These results suggest that the ERK pathway might be important for the up-regulation of RANKL protein in osteoblasts.

Figure 2. Effect of Ang II on RANKL expression in human osteoblasts. *A*) Quantification of RANKL and OPG mRNA expression by real-time PCR. Human osteoblasts were treated with Ang II (1×10^{-6} M) with or without an Ang II type 1 receptor blocker (ARB) (olmesartan; 1×10^{-5} M) or an Ang II type 2 receptor blocker[PD123329 (PD); 1×10^{-5} M] for 24 h. $^*P < 0.01$ *vs.* no treatment; $^\dagger P < 0.01$ *vs.* Ang II; $n = 6–8$ per group. *B, C*) Effect of Ang II on RANKL expression in human osteoblasts, assessed by (*B*) soluble RANKL concentration and (*C*) Western blotting with anti-RANKL antibody. Human osteoblasts were treated with vitamin D3 (Vit.D3) (1×10^{-8} M) or Ang II (1×10^{-6} M) with or without an Ang II type 1 receptor blocker (olmesartan; 1×10^{-5} M) or an Ang II type 2 receptor blocker (PD123329; 1×10^{-5} M) for 48 h. $^*P < 0.01$ *vs.* no treatment; $^\dagger P < 0.01$ *vs.* Ang II; $n = 6–8$ per group. *D*) Effect of Ang II on OPG expression in human osteoblasts. Human osteoblasts were treated with vitamin D_3 (1×10^{-8} M) or Ang II (1×10^{-6} M) with or without an Ang II type 1 receptor blocker (olmesartan; 1×10^{-5} M) or an Ang II type 2 receptor blocker (PD123329; 1×10^{-5} M) for 48 h. $^*P < 0.01$ *vs.* no treatment; $^\dagger P < 0.01$ *vs.* Ang II; $n = 6$ per group. *E*) Ang II activated ERK, p38 MAPK, and Akt in human osteoblasts. Representative Western blot of phospho-specific (P) -ERK, ERK, P-p38 MAPK, p38 MAPK, P-Akt, or Akt in human osteoblasts. Human osteoblasts were treated with Ang II (1×10^{-6} M) with or without pretreatment (1 h before) with an Ang II type 1 receptor blocker (olmesartan; 1×10^{-5} M) or an Ang II type 2 receptor blocker (PD123329; 1×10^{-5} M) for 10 min. *F*) Inhibition of ERK, p38 MAPK, and Akt by specific inhibitors on soluble RANKL concentration in human osteoblasts. Effect of an Ang II type 1 receptor blocker (olmesartan; 1×10^{-5} M), an MEK inhibitor (U0126; 50 μM), a p38 MAPK inhibitor (SB203580; 10 μM), and a PI3K inhibitor (wortmannin; 100 nM) in a soluble RANKL concentration in human osteoblasts. $^*P < 0.01$ *vs.* control; $^\dagger P < 0.01$ *vs.* Ang II; $n = 8$ per group. *G*) Evaluation of Ang II-induced RANKL up-regulation on TRAP activity in a coculture system with human osteoblasts and osteoclast precursors. Representative phase-contrast microscopic views show the differentiation of osteoclasts induced by vitamin D_3 (1×10^{-8} M) or Ang II (1×10^{-6} M) with or without an Ang II type 1 receptor blocker (olmesartan; 1×10^{-5} M), an MEK inhibitor (U0126; 50 μM), a p38 MAPK inhibitor [SB203580 (SB); 10 μM], and a PI3K inhibitor [wortmannin (Wor); 100 nM], with TRAP staining (top panel) and Hoechst 33258 staining (bottom panel) (×100). *H*) Evaluation of Ang II-induced RANKL up-regulation on TRAP activity in a coculture system with human osteoblasts and osteoclast precursors transfected with siRNA for RANK. Representative phase-contrast microscopic views show the differentiation of osteoclasts induced by Ang II (1×10^{-6} M) with siRNA for scramble or RANK, with TRAP staining (top panel) and Hoechst 33258 staining (bottom panel) (×40). Con, control.

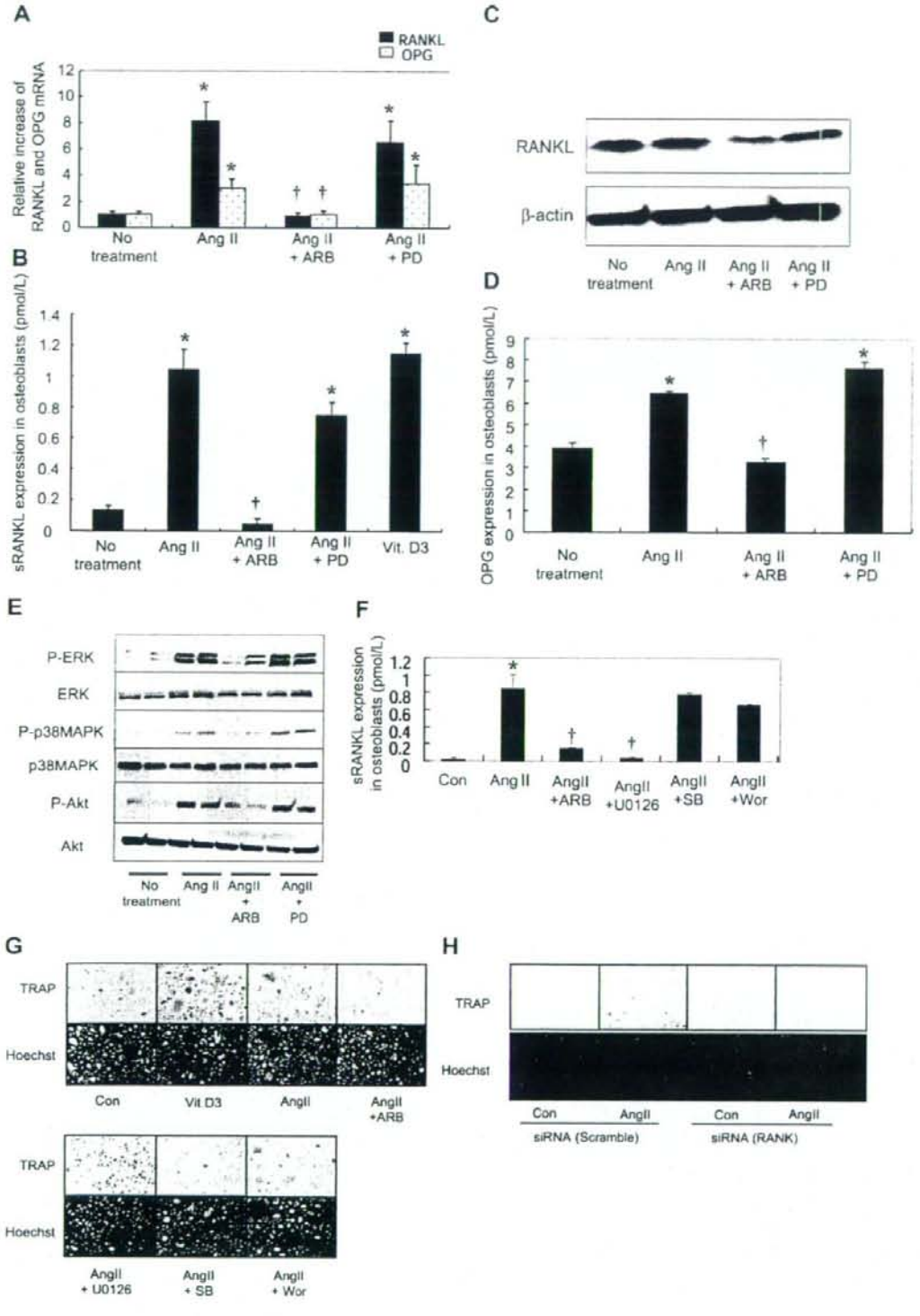
A
RANKL
OPG
Relative increase of RANKL and OPG mRNA
No treatment
Ang II
Ang II + ARB
Ang II + PD
B
sRANKL expression in osteoblasts (pmol/L)
No treatment
Ang II
Ang II + ARB
Ang II + PD
Vit. D3
C
RANKL
β-actin
No treatment
Ang II
Ang II + ARB
Ang II + PD
D
OPG expression in osteoblasts (pmol/L)
No treatment
Ang II
Ang II + ARB
Ang II + PD
E
P-ERK
ERK
P-p38MAPK
p38MAPK
P-Akt
Akt
No treatment
Ang II
AngII + ARB
AngII + PD
F
sRANKL expression in osteoblasts (pmol/L)
Con
Ang II
AngII +ARB
AngII +U0126
AngII +SB
AngII +Wor
G
TRAP
Hoechst
Con
Vit D3
AngII
AngII +ARB
AngII + U0126
AngII + SB
AngII + Wor
H
TRAP
Hoechst
Con
AngII
siRNA (Scramble)
siRNA (RANK)

To further confirm the involvement of the RANKL-RANK pathway in Ang II-induced osteoclasts differentiation, we designed the siRNA for RANK to knockdown its expression. We successfully inhibited its expression (87% inhibition) in human osteoclast precursors by Nucleofector transfection (13). To clarify the contribution of RANK in Ang II-induced osteoclast differentiation, we cocultured the siRNA transfected-osteoclast precursors with human osteoblasts with or without treatment with Ang II. Indeed, Ang II-induced TRAP-positive multinuclear cells were completely abolished in RANK siRNA transfected cells (Fig. 2*H*). These results suggest that Ang II-induced osteoclast differentiation may be mediated by the RANK-RANKL system.

In vivo effects of Ang II on osteoporosis in rat ovariectomy model

To further clarify the effect of Ang II on the differentiation of osteoclasts, we established a rat ovariectomy model of estrogen deficiency as a model of osteoporosis with or without systemic administration of Ang II at a subpresser dose (200 ng/kg/min). At 28 days after bilateral ovariectomy, the serum estradiol level was significantly decreased in the ovariectomy group, whereas there was no significant difference in body weight, consistent with our previous report (11). We examined both TRAP and ALP activity to evaluate the total balance of osteoclast and osteoblast activity in the process of osteoporosis. TRAP activity was significantly increased in the tibiae of ovariectomized rats with systemic administration of Ang II (**Fig. 3*A***). Indeed, the TRAP-positive stained area was also increased in the tibiae of OVX rats with systemic administration of Ang II (Fig. 3*B*). Although ALP activity was also increased in the tibiae of OVX rats by Ang II (Fig. 3*C*), the ratio of ALP to TRAP was significantly decreased in the tibiae of OVX rats by Ang II (Fig. 3*D*). These results suggest that Ang II accelerated the turnover of bone metabolism, which is similar to the typical pattern in elderly postmenopausal women who are at high risk for osteoporosis. Of importance, bone density as assessed by DEXA was significantly decreased in the tibiae of OVX rats by Ang II (Fig. 3*E*). These results were accompanied by a change in urinary deoxypyridinoline, which is released from bone by the processing of tissue collagen. Treatment with Ang II significantly induced the ovariectomy-induced increase in urinary deoxypyridinoline (Fig. 3*F*). These results suggest that Ang II directly accelerated estrogen deficiency-induced osteoporosis independent of blood pressure.

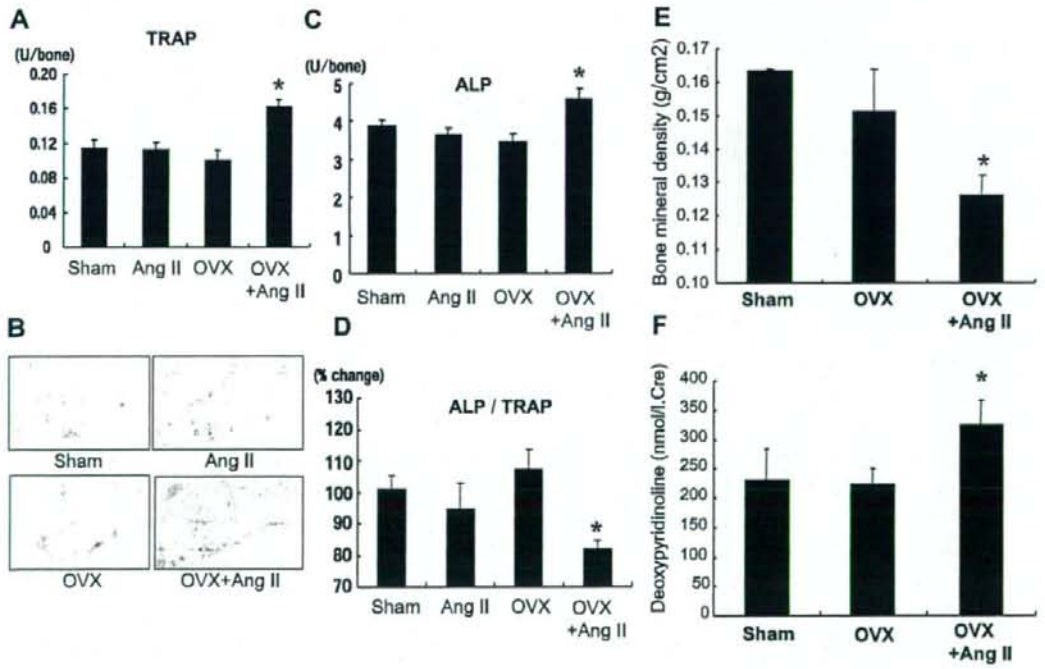

Figure 3. Effects of Ang II infusion in ovariectomy-induced osteoporosis rat model. *A*) TRAP activity. *B*) TRAP staining. *C*) ALP activity. *D*) Ratio of ALP to TRAP activity. *E*) Bone marrow density by DEXA. *F*) Urinary deoxypyridinoline after 28 days of each treatment. Sham, sham operation; Ang II, infusion of Ang II (200 ng/kg/min); OVX, bilateral ovariectomy; OVX + Ang II, bilateral ovariectomy and treatment with Ang II (200 ng/kg/min); U, release of 1 μmol of *p*-nitrophenol/min. Urinary deoxypyridinoline was adjusted for urinary creatinine concentration. $*P < 0.05$ *vs.* sham; $n = 6–10$ per group.

Ang II type 1 receptor blocker ameliorates ovariectomy-induced osteoporosis

To clarify the role of Ang II and high blood pressure in bone metabolism further, we used an ovariectomy model of estrogen deficiency in a hypertensive model, SHRs. At 28 days after bilateral ovariectomy, TRAP activity was significantly increased in the tibiae of OVX SHRs compared with sham-operated SHRs (**Fig. 4*A, B***). Because ALP activity was not changed in the tibiae of OVX SHRs (Fig. 4*C*), the ratio of ALP to TRAP was significantly decreased in the tibiae of OVX SHRs compared with that in sham-operated rats (Fig. 4*D*). Of importance, TRAP and ALP activities were not increased in ovariectomized normotensive WKYs (TRAP activity, sham: 0.074±0.006, ovariectomy: 0.076±0.008; ALP activity, sham: 2.108±0.121, ovariectomy: 2.203±0.183). These results indicate that osteoclasts would be activated in SHRs but not in WKYs with ovariectomy, leading to worse osteoporosis.

Because tissue Ang II is well known to be increased in SHRs, we further examined whether an Ang II type 1 receptor blocker, olmesartan, would ameliorate ovariectomy-induced osteoporosis in SHRs. Blood pressure was decreased with continuous administration of olmesartan (0.5, 1, or 3 mg/kg/day by osmotic pump) and

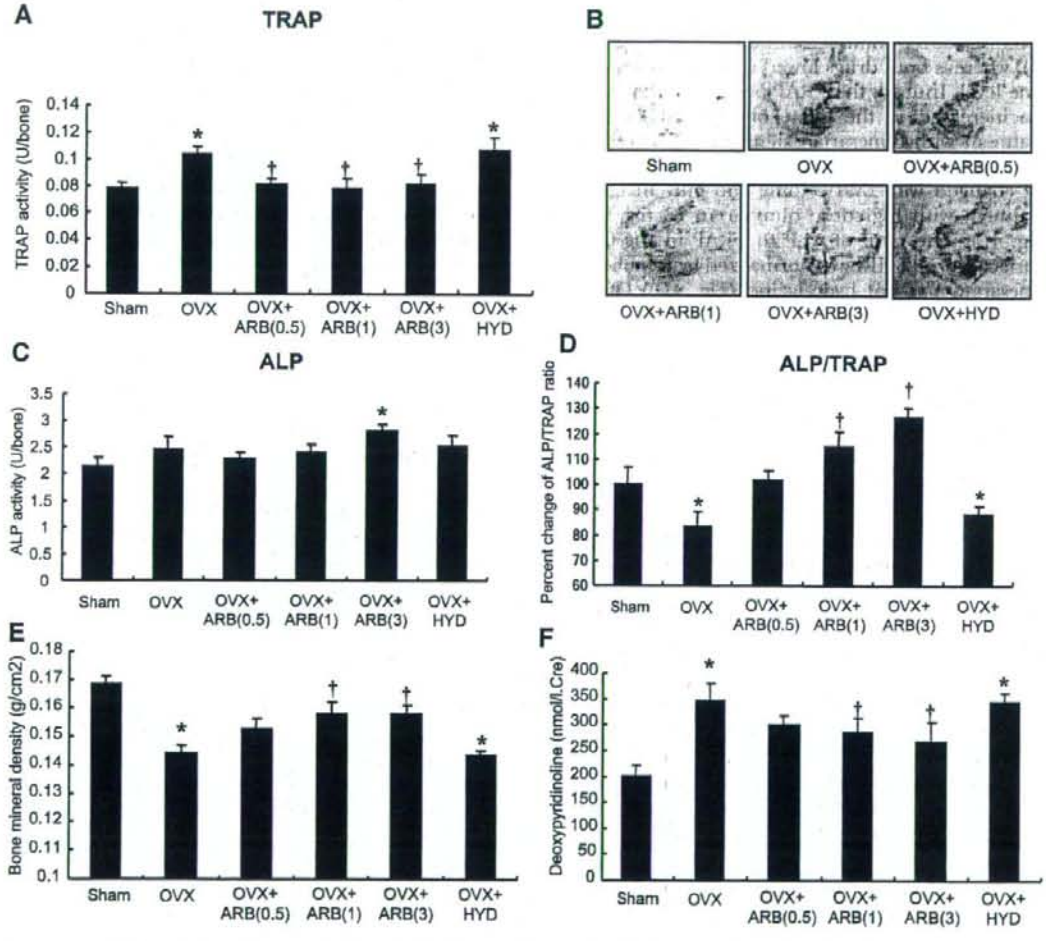

Figure 4. Effects of an Ang II type 1 receptor blocker (ARB), olmesartan, in the ovariectomy-induced osteoporosis SHR model. *A*) TRAP activity. *B*) TRAP staining. *C*) ALP activity. *D*) Ratio of ALP to TRAP activity. *E*) Bone mineral density by DEXA. *F*) Urinary deoxypyridinoline after 28 days of each treatment. Sham, sham operation; OVX, bilateral ovariectomy; OVX + ARB (0.5), bilateral ovariectomy and treatment with olmesartan (0.5 mg/kg/day); OVX + ARB (1), bilateral ovariectomy and treatment with olmesartan (1 mg/kg/day); OVX + ARB (3), bilateral ovariectomy and treatment with olmesartan (3 mg/kg/day); OVX + HYD, bilateral ovariectomy and treatment with hydralazine (10 mg/kg/day in drinking water); U, release of 1 μmol of *p*-nitrophenol/min. Urinary deoxypyridinoline was adjusted for urinary creatinine (Cre) concentration. $^{*}P < 0.05$ *vs.* sham; $^{\dagger}P < 0.05$ *vs.* OVX; $n = 6$–10 per group.

TABLE 1. *Physiological parameters of each group in SHRs*

Group	Body weight (g)	Systolic blood pressure (mmHg)	Heart rate (beats/min)
Sham	230.1 ± 8.1	138 ± 3.8	364 ± 4.7
OVX	250.9 ± 8.8	132 ± 9.4	381 ± 10.6
OVX + ARB (0.5)	253.8 ± 8.3	107 ± 5.8*	352 ± 10.2
OVX + ARB (1)	239.6 ± 5.8	88 ± 2.6*	359 ± 5.8
OVX + ARB (3)	243.3 ± 6.8	70 ± 3.4*	364 ± 5.5
OVX + HYD	240.2 ± 8.1	91 ± 2.3*	306 ± 5.3

Values are means ± SE. ARB (0.5, 1, or 3), angiotensin receptor blockade with olmesartan, (0.5, 1, or 3 mg/kg/day); HYD, hydralazine (10 mg/kg/day). *$P < 0.05$ *vs.* OVX.

hydralazine (10 mg/kg/day in drinking water), as shown in **Table 1**. Ovariectomy-induced TRAP activity in SHRs was significantly ameliorated by continuous administration of olmesartan but not hydralazine (Fig. 4*A*), whereas both drugs lowered blood pressure to the same level. Indeed, the TRAP-positive stained area was also increased in the tibiae of OVX SHRs, whereas treatment with olmesartan significantly decreased the TRAP-positive stained area (Fig. 4*B*). ALP activity was not changed with ovariectomy and only increased by treatment with high-dose olmesartan (3 mg/kg/day) (Fig. 4*C*). The ratio of ALP to TRAP in the tibiae of ovariectomized SHRs was normalized by treatment with olmesartan but not hydralazine (Fig. 4*D*). Of importance, these results were accompanied by a significant increase in bone mineral density, as assessed by DEXA, in the tibiae of OVX SHRs (Fig. 4*E*). The increase in urinary deoxypyridinoline induced by ovariectomy in SHRs was consistently significantly attenuated by olmesartan but not by hydralazine (Fig. 4*F*). These results suggest that an Ang II type 1 receptor blocker attenuated osteoporosis induced by estrogen deficiency and high blood pressure.

Furthermore, we used AT_{1A} KO mice to examine the contribution of Ang II in the process of osteoporosis. It was reported that there was no gross abnormality in bone development or osteoporosis in AT_{1A} KO mice, although arterial pressure was reduced (20). Because amounts of circulating and tissue Ang II are elevated in the five-sixths nephrectomy hypertensive model with a significant increase in systolic blood pressure, we developed an Ang II-dependent osteoporosis model by ovariectomy and five-sixths nephrectomy. In the evaluation of physical characteristics, AT_{1A} KO mice showed a decrease in arterial blood pressure compared with wild-type mice, whereas treatment with ovariectomy and five-sixths nephrectomy increased arterial blood pressure in wild-type mice but not in AT_{1A} KO mice (**Table 2**). In ovariectomized and five-sixths nephrectomized mice, computed tomography indicated that bone volume and bone thickness were significantly decreased, whereas bone trabecular space was significantly increased compared with that in sham-operated mice (**Fig. 5*A*, *B***). In contrast, in AT_{1A} KO mice, there was no difference in these markers between sham operation and ovariectomy/nephrectomy (Fig. 5*A*, *B*). The histology of the proximal tibia showed that TRAP-positive cells were significantly increased in OVX/nephrectomized wild-type mice but not in AT_{1A} KO mice (Fig. 5*C*). The increase in urinary deoxypyridinoline induced by ovariectomy/nephrectomy was consistently observed in wild-type mice but not in AT_{1A} KO mice (Fig. 5*D*).

DISCUSSION

Clinical epidemiological evidence has demonstrated that high blood pressure is associated with an increase in bone loss, especially in elderly women. Systemic blood pressure is a significant predictor of bone mineral loss in the femoral neck. It is known that high blood pressure is associated with abnormalities of calcium metabolism, including an increase in urinary calcium excretion for a given sodium intake and evidence of a secondary increase in parathyroid gland activity (22). Sustained hypercalciuria in patients with high blood pressure leads to an increased risk of bone mineral loss, with a negative association between blood pressure and bone mineral density (23, 24). Thiazides are thought to protect against age-related bone loss by

TABLE 2. *Physiological parameters of each group in wild-type and AT1R KO mice*

Group	Body weight (g)	Systolic blood pressure (mmHg)	Heart rate (beats/min)
Wild-type (sham)	18.1 ± 0.4	94 ± 2.4	415 ± 30.3
Wild-type (OVX+five-sixths nephrectomy)	18.5 ± 0.21	119 ± 2.5*	540 ± 13.7
AT1R KO (sham)	18.9 ± 1.43	59 ± 1.9*	435 ± 14.4
AT1R KO (OVX+five-sixths nephrectomy)	17.7 ± 0.32	65 ± 2.4*	402 ± 30.9

Values are means ± SE. *$P < 0.05$ *vs.* wild (sham)

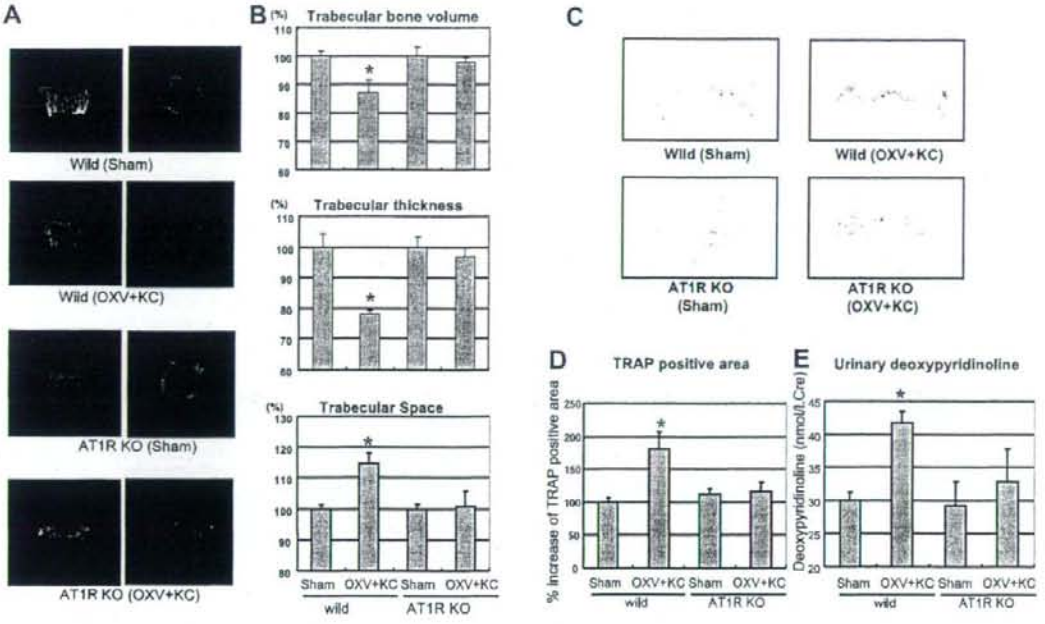

Figure 5. Effects of hypertension on bone metabolism in OVX wild-type (Wild) mice and AT_{1A} KO mice. *A*) Microcomputed tomography three-dimensional image of the trabecular architecture of the proximal tibia metaphysic in sham operation (Sham) and ovariectomy and five-sixths nephrectomy (OVX+KC) of wild-type or AT_{1A} KO mice. *B*) Change of trabecular bone parameters of mouse proximal tibia metaphysic analyzed by microcomputed tomography in sham operation and ovariectomy and five-sixths nephrectomy of wild-type or AT_{1A} KO mice. $*P < 0.05$ *vs.* sham; $n = 6$ per group. *C*) TRAP staining. *D*) Quantification of the TRAP-positive staining area in cancerous bone under the growth plate. *E*) Urinary deoxypyridinoline in sham operation and ovariectomy and five-sixths nephrectomy of wild-type or AT_{1A} KO mice. $*P < 0.05$ *vs.* sham; $n = 6$ per group.

reducing urinary calcium excretion (25). In the kidney, thiazides act at the distal convoluted tubule by blocking the coupled resorption of Na and Cl through the thiazide-sensitive Na/Cl cotransporter. This effect triggers a Na/Ca exchanger promoting calcium influx and sodium efflux, leading to a decrease in parathyroid hormone, a mild increase in serum calcium level, and a decrease in bone turnover. In a prospective cohort study, use of thiazides for more than 365 days was associated with a decreased risk of hip fracture (4). Although this association may reflect calcium loss associated with high blood pressure, there are few reports clarifying the role of hypertension in osteoporosis. From this viewpoint, we focused on the role of Ang II in osteoporosis. Interestingly, subanalysis of a retrospective case-control study in a large population (30,601 fractures and 120,819 controls) of men and women with ages ranging from 30 to 79 yr has recently shown that use of ACE inhibitors significantly reduced the risk of fractures. However, calcium channel blockers had no effect on the risk of fractures in the present study, and thus far there has been no evidence of the value of calcium channel blockers for treatment of osteoporosis associated with hypertension. Thus, it is noteworthy that the present study demonstrated that Ang II regulated the bone metabolism of osteoblasts and osteoclasts, which potentially contributes to osteoporosis in hypertensive patients.

The local renin-angiotensin system plays an important role in the regulation of tissue remodeling in several tissues. Ang II has been postulated to be able to act on the cells involved in bone metabolism through receptors located in osteoblasts and osteoclasts or regulation of flow in bone marrow capillaries. Hatton *et al.* (8) indicated that Ang I and II were potent stimulators of osteoclastic bone resorption. On the contrary, Ang II stimulates the proliferation of osteoblast-rich populations of cells (9). Osteoclasts originate from monocyte/macrophage lineage multinucleated cells, which can also be the target of Ang II. Osteoblasts/stromal cells express RANKL in response to several bone-resorbing factors including vitamin D_3 to support osteoclast differentiation from their precursors. Osteoclast precursors, which express RANK, recognize RANKL through cell-to-cell interactions with osteoblasts/stromal cells and differentiate into mature osteoclasts in the presence of M-CSF. Targeted disruption of either RANKL or RANK in mice causes a lack of osteoclasts and an osteopetrotic phenotype (26). Of note, the present study clearly demonstrated that Ang II indirectly promoted the differentiation and activation of osteoclasts responsible for bone resorption *via* up-regulation of

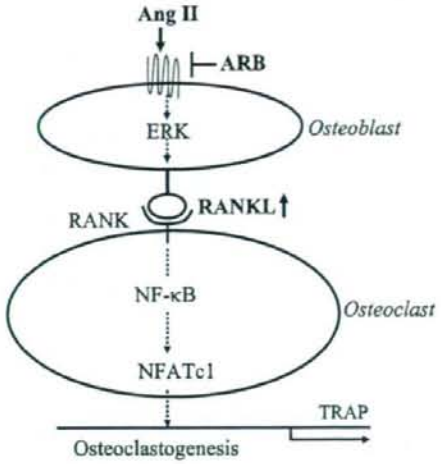

Figure 6. Summary scheme of angiotensin II-induced osteoclastogenesis. Osteoclast precursors with RANK (receptor) recognize RANKL (ligand) of osteoblast by cell-cell contact and differentiate into mature osteoclasts. The transcription factor, NFκB, plays a pivotal role in the activation of nuclear factor of activated T cells c1 (NFATc1), which regulates osteoclastogenesis assessed by TRAP activity. Ang II increases RANKL expression in osteoblasts, whereas the angiotensin receptor blockade (ARB) ameliorates osteoclastogenesis through down-regulation of RANKL expression.

RANKL in osteoblasts. We also confirm that treatment with Ang II activated NFκB in osteoclasts (data not shown). Thus, the renin-angiotensin system could be involved in the regulation of osteoclast activation. As osteoclast differentiation is regulated by a variety of hormones, local factors, and inflammatory cytokines, such as interleukin-1 and tumor necrosis factor-α (26, 27), the renin-angiotensin system is a novel component of the osteoclast differentiation system (**Fig. 6**). On the other hand, locally elevated extracellular calcium levels have been suggested to play roles in regulation of bone remodeling (28, 29), and MAPK pathways mediate the modulation of the cellular responses by high extracellular calcium (30). Previous reports demonstrated that ERK would be involved mainly in induction of RANKL by high extracellular signaling, but not PI3K or p38 MAPK, by using these specific inhibitors (31). Although it was known that intracellular signaling of Ang II *via* the Ang II type 1 receptor might be coupled with calcium reflex, especially inducing release of intracellular calcium (32), our results also suggested that treatment of Ang II in osteoblasts up-regulated RANKL expression through the ERK pathway, which led to osteoclast activation and differentiation. Alternatively, Ang II also regulates local blood flow in bone marrow capillaries. As hypertension decreases local blood flow in microvessels, blockade of the renin-angiotensin system may improve tissue blood flow in bone marrow capillaries, enhancing bone marrow formation.

In this study, we established two rat models and one mouse model with ovariectomy as osteoporosis models corresponding to elderly women in a state of estrogen withdrawal. Interestingly, continuous administration of Ang II accelerated osteoclast activation induced by estrogen deficiency. It has been reported that estrogen antagonizes the bioactive effect of Ang II through signaling cross-talk in vascular smooth muscle cells (33, 34). Previous reports suggested that administration of an ACE inhibitor, enalapril, and an angiotensin II antagonist, losartan, had no effect on bone metabolism in normal rats (35). The difference from the present study might be due to the different model (normotension *vs.* SHR or Ang II infusion) or high affinity to the Ang II receptor (losartan *vs.* olmesartan). More strong evidence about the contribution of Ang II to osteoporosis is that both hypertension and ovariectomy induced the symptoms of osteoporosis in wild-type mice but not in AT_{1A} KO mice.

As osteoporosis is the main cause of bone fractures in postmenopausal women and elderly individuals and is associated with pain, deformity, and loss of independence (36), the present study suggests new therapeutic aspects of antihypertensive drugs, Ang II receptor blockers, to treat elderly hypertensive patients, especially the female population. Because of the increasing number of elderly people and the increase in the prevalence of osteoporosis, the need for focused preventive strategies has become a public health priority. Peak bone mass attained in the first 20 yr of life and the rate at which bone is lost in later years are the most important factors influencing the occurrence of osteoporosis. Because Ang II caused osteoclast activation, leading to accelerated osteoporosis, angiotensin receptor blockers could lessen the risk of osteoporosis in elderly people, possibly beyond their blood pressure-lowering effect. Further clinical trials using Ang II receptor blockers are necessary to confirm this concept.

This work was partially supported by the National Institute of Biomedical Innovation, by a grant-in-aid from the Ministry of Public Health and Welfare, by a grant-in-aid from Japan Promotion of Science, and through Special Coordination Funds of the Ministry of Education, Culture, Sports, Science and Technology, the Japanese Government. We thank Miss Natsuki Yasumasa for technical support.

REFERENCES

1. Resnick, L. M., Laragh, J. H., Sealey, J. E., and Alderman, M. H. (1983) Divalent cations in essential hypertension: relations between serum ionized calcium, magnesium, and plasma renin activity. *N. Engl. J. Med.* **309**, 888–891
2. Cappuccio, F. P., Kalaitzidis, R., Duneclift, S., and Eastwood, J. B. (2000) Unravelling the links between calcium excretion, salt intake, hypertension, kidney stones and bone metabolism. *J. Nephrol.* **13**, 169–177
3. Reid, I. R., Ames, R. W., Orr-Walker, B. J., Clearwater, J. M., Horne, A. M., Evans, M. C., Murray, M. A., McNeil, A. R., and Gamble, G. D. (2000) Hydrochlorothiazide reduces loss of cortical bone in normal postmenopausal women: a randomized controlled trial. *Am. J. Med.* **109**, 362–370
4. Schoofs, M. W., van der Klift, M., Hofman, A., de Laet, C. E., Herings, R. M., Stijnen, T., Pols, H. A., and Stricker, B. H.

(2003) Thiazide diuretics and the risk for hip fracture. *Ann. Intern. Med.* **139,** 476–482
5. Schlienger, R. G., Kraenzlin, M. E., Jick, S. S., and Meier, C. R. (2004) Use of β-blockers and risk of fractures. *JAMA* **292,** 1326–1332
6. Lynn, H., Kwok, T., Wong, S. Y., Woo, J., and Leung, P. C. (2006) Angiotensin converting enzyme inhibitor use is associated with higher bone mineral density in elderly Chinese. *Bone* **38,** 584–588
7. Rejnmark, L., Vestergaard, P., and Mosekilde, L. (2006) Treatment with β-blockers, ACE inhibitors, and calcium-channel blockers is associated with a reduced fracture risk: a nationwide case-control study. *J. Hypertens.* **24,** 581–589
8. Hatton, R., Stimpel, M., and Chambers, T. J. (1997) Angiotensin II is generated from angiotensin I by bone cells and stimulates osteoclastic bone resorption in vitro. *J. Endocrinol.* **152,** 5–10
9. Hiruma, Y., Inoue, A., Hirose, S., and Hagiwara, H. (1997) Angiotensin II stimulates the proliferation of osteoblast-rich populations of cells from rat calvariae. *Biochem. Biophys. Res. Commun.* **230,** 176–178
10. Shimizu, H., Sakamoto, M., and Sakamoto, S. (1990) Bone resorption by isolated osteoclasts in living versus devitalized bone: differences in mode and extent and the effects of human recombinant tissue inhibitor of metalloproteinases. *J. Bone Miner. Res.* **5,** 411–418
11. Shimizu, H., Nakagami, H., Tsukamoto, I., Morita, S., Kunugiza, Y., Tomita, T., Yoshikawa, H., Kaneda, Y., Ogihara, T., and Morishita, R. (2006) NFκB decoy oligodeoxynucleotides ameliorates osteoporosis through inhibition of activation and differentiation of osteoclasts. *Gene Ther.* **13,** 933–941
12. Nakagami, H., Morishita, R., Yamamoto, K., Taniyama, Y., Aoki, M., Kim, S., Matsumoto, K., Nakamura, T., Higaki, J., and Ogihara, T. (2000) Anti-apoptotic action of hepatocyte growth factor through mitogen-activated protein kinase on human aortic endothelial cells. *J. Hypertens.* **18,** 1411–1420
13. Taylor, A., Rogers, M. J., Tosh, D., and Coxon, F. P. (2007) A novel method for efficient generation of transfected human osteoclasts. *Calcif. Tissue Int.* **80,** 132–136
14. Yasuda, H., Shima, N., Nakagawa, N., Yamaguchi, K., Kinosaki, M., Mochizuki, S., Tomoyasu, A., Yano, K., Goto, M., Murakami, A., Tsuda, E., Morinaga, T., Higashio, K., Udagawa, N., Takahashi, N., and Suda, T. (1998) Osteoclast differentiation factor is a ligand for osteoprotegerin/osteoclastogenesis-inhibitory factor and is identical to TRANCE/RANKL. *Proc. Natl. Acad. Sci. U. S. A.* **95,** 3597–3602
15. Nakagami, H., Takemoto, M., and Liao, J. K. (2003) NADPH oxidase-derived superoxide anion mediates angiotensin II-induced cardiac hypertrophy. *J. Mol. Cell. Cardiol.* **35,** 851–859
16. Venken, K., Boonen, S., Van Herck, E., Vandenput, L., Kumar, N., Sitruk-Ware, R., Sundaram, K., Bouillon, R., and Vanderschueren, D. (2005) Bone and muscle protective potential of the prostate-sparing synthetic androgen 7α-methyl-19-nortestosterone: evidence from the aged orchidectomized male rat model. *Bone* **36,** 663–670
17. Xiang, A., Kanematsu, M., Kumar, S., Yamashita, D., Kaise, T., Kikkawa, H., Asano, S., and Kinoshita, M. (2007) Changes in micro-CT 3D bone parameters reflect effects of a potent cathepsin K inhibitor (SB-553484) on bone resorption and cortical bone formation in ovariectomized mice. *Bone* **40,** 1231–1237
18. Sone, T., Tamada, T., Jo, Y., Miyoshi, H., and Fukunaga, M. (2004) Analysis of three-dimensional microarchitecture and degree of mineralization in bone metastases from prostate cancer using synchrotron microcomputed tomography. *Bone* **35,** 432–438
19. Parfitt, A. M., Mathews, C. H., Villanueva, A. R., Kleerekoper, M., Frame, B., and Rao, D. S. (1983) Relationships between surface, volume, and thickness of iliac trabecular bone in aging and in osteoporosis: implications for the microanatomic and cellular mechanisms of bone loss. *J. Clin. Invest.* **72,** 1396–1409
20. Sugaya, T., Nishimatsu, S., Tanimoto, K., Takimoto, E., Yamagishi, T., Imamura, K., Goto, S., Imaizumi, K., Hisada, Y., Otsuka, A., Uchida, H., Sugiura, M., Fukuta, K., Fukamizu, A., and Murakami, K. (1995) Angiotensin II type 1a receptor-deficient mice with hypotension and hyperreninemia. *J. Biol. Chem.* **270,** 18719–18722
21. Ibrahim, H. N., and Hostetter, T. H. (1998) The renin-aldosterone axis in two models of reduced renal mass in the rat. *J. Am. Soc. Neurol.* **9,** 72–76
22. McCarron, D. A., Pingree, P. A., Rubin, R. J., Gaucher, S. M., Molitch, M., and Krutzik, S. (1980) Enhanced parathyroid function in essential hypertension: a homeostatic response to a urinary calcium leak. *Hypertension* **2,** 162–168
23. MacGregor, G. A., and Cappuccio, F. P. (1993) The kidney and essential hypertension: a link to osteoporosis? *J. Hypertens.* **11,** 781–785
24. McCarron, D. A. (1982) Low serum concentrations of ionized calcium in patients with hypertension. *N. Engl. J. Med.* **307,** 226–228
25. Duarte, C. G., Winnacker, J. L., Becker, K. L., and Pace, A. (1971) Thiazide-induced hypercalcemia. *N. Engl. J. Med.* **284,** 828–830
26. Kong, Y. Y., Yoshida, H., Sarosi, I., Tan, H. L., Timms, E., Capparelli, C., Morony, S., Oliveira-dos-Santos, A. J., Van, G., Itie, A., Khoo, W., Wakeham, A., Dunstan, C. R., Lacey, D. L., Mak, T. W., Boyle, W. J., and Penninger, J. M. (1999) OPGL is a key regulator of osteoclastogenesis, lymphocyte development and lymph-node organogenesis. *Nature* **397,** 315–323
27. Van der Pluijm, G., Most, W., van der Wee-Pals, L., de Groot, H., Papapoulos, S., and Lowik, C. (1991) Two distinct effects of recombinant human tumor necrosis factor-α on osteoclast development and subsequent resorption of mineralized matrix. *Endocrinology* **129,** 1596–1604
28. Kaji, H., Sugimoto, T., Kanatani, M., and Chihara, K. (1996) High extracellular calcium stimulates osteoclast-like cell formation and bone-resorbing activity in the presence of osteoblastic cells. *J. Bone Miner. Res.* **11,** 912–920
29. Kameda, T., Mano, H., Yamada, Y., Takai, H., Amizuka, N., Kobori, M., Izumi, N., Kawashima, H., Ozawa, H., Ikeda, K., Kameda, A., Hakeda, Y., and Kumegawa, M. (1998) Calcium-sensing receptor in mature osteoclasts, which are bone resorbing cells. *Biochem. Biophys. Res. Commun.* **245,** 419–422
30. Yamaguchi, T., Chattopadhyay, N., Kifor, O., Sanders, J. L., and Brown, E. M. (2000) Activation of p42/44 and p38 mitogen-activated protein kinases by extracellular calcium-sensing receptor agonists induces mitogenic responses in the mouse osteoblastic MC3T3-E1 cell line. *Biochem. Biophys. Res. Commun.* **279,** 363–368
31. Kim, Y. H., Kim, J. M., Kim, S. N., Kim, G. S., and Baek, J. H. (2008) p44/42 MAPK activation is necessary for receptor activator of nuclear factor-κB ligand induction by high extracellular calcium. *Biochem. Biophys. Res. Commun.* **304,** 729–735
32. Inagami, T., Eguchi, S., Numaguchi, K., Motley, E. D., Tang, H., Matsumoto, T., and Yamakawa, T. (1999) Cross-talk between angiotensin II receptors and the tyrosine kinases and phosphatases. *J. Am. Soc. Neurol.* **10**(Suppl. 11), S57–S61
33. Takeda-Matsubara, Y., Nakagami, H., Iwai, M., Cui, T. X., Shiuchi, T., Akishita, M., Nahmias, C., Ito, M., and Horiuchi, M. (2002) Estrogen activates phosphatases and antagonizes growth-promoting effect of angiotensin II. *Hypertension* **39,** 41–45
34. Liu, H. W., Iwai, M., Takeda-Matsubara, Y., Wu, L., Li, J. M., Okumura, M., Cui, T. X., and Horiuchi, M. (2002) Effect of estrogen and AT1 receptor blocker on neointima formation. *Hypertension* **40,** 451–457; discussion 448–450
35. Broulik, P. D., Tesar, V., Zima, T., and Jirsa, M. (2001) Impact of antihypertensive therapy on the skeleton: effects of enalapril and AT1 receptor antagonist losartan in female rats. *Physiol. Res.* **50,** 353–358
36. Riggs, B. L., and Melton, L. J., 3rd (1992) The prevention and treatment of osteoporosis. *N. Engl. J. Med.* **327,** 620–627

Received for publication October 9, 2007.
Accepted for publication January 10, 2008.